BRNO UNIVERSITY OF TECHNOLOGY
VYSOKÉ UČENÍ TECHNICKÉ V BRNĚ

CENTRAL EUROPEAN INSTITUTE OF TECHNOLOGY BUT
STŘEDOEVROPSKÝ TECHNOLOGICKÝ INSTITUT VUT

RESEARCH AND DEVELOPMENT OF A TECHNOLOGY OF HARD ANODIZATION OF NONFERROUS ALLOYS

VÝZKUM A VÝVOJ TECHNOLOGIE PŘÍPRAVY TVRDÉ ANODIZACE NEŽELEZNÝCH SLITIN

SHORT VERSION OF DOCTORAL THESIS
TEZE DIZERTAČNÍ PRÁCE

AUTHOR
AUTOR PRÁCE
Ing. Michaela Remešová

SUPERVISOR
ŠKOLITEL
prof. Ing. Jozef Kaiser, Ph.D.

BRNO 2020

Abstract

The thesis is focused on the research and development of the technological process for the preparation of hard anodic coatings on three different non-ferrous materials, namely (i) aluminium alloy (AA1050), (ii) pure magnesium (99.9% Mg), and (iii) zinc alloy (ZnTi2). Suitable combinations of anodizing conditions (voltage, current density, temperature and composition of the electrolyte, etc.) can produce anodic coatings with different properties. The effect of pre-treatment and anodizing conditions on the appearance, morphology, thickness and hardness of the produced anodic coatings was demonstrated in the present thesis. In order to increase tribological properties and hardness, the anodic coatings were directly doped with Al_2O_3 or with a mixture of Al_2O_3/PTFE particles during the anodizing process. The theoretical part describes the basic principles of anodization, the methods used in industry and the technological process. The experimental part is divided into three basic parts. The first part is devoted to anodizing of aluminium alloy. The second part is focused on anodizing of pure magnesium, and the last part is focused on anodizing of zinc alloy, which has not been researched as thoroughly as anodizing of aluminium.

Keywords

Surface treatment, anodizing process, aluminium, magnesium, zinc, coating microstructure, hardness, wear

Abstrakt

Práce je zaměřena na výzkum a vývoj technologie přípravy tvrdých anodických vrstev na třech různých typech neželezných materiálů a to (i) hliníkové slitině (AA1050), (ii) čistém hořčíku (99.9% Mg) a (iii) zinkové slitině (ZnTi2). Vhodnou kombinací anodizačních podmínek (napětí, proudová hustota, teplota a složení elektrolytu atd.) lze vytvářet anodické vrstvy s rozdílnými vlastnostmi. V rámci předložené práce byl prokázán vliv předúpravy a anodizačních podmínek na vzhled, morfologii, tloušťku a tvrdost vytvořených anodických vrstev. Pro zvýšení tribologických vlastností a tvrdosti byly anodické vrstvy přímo dopovány Al_2O_3 částicemi nebo kombinací Al_2O_3 a PTFE částic během anodizačního procesu. Teoretická část práce popisuje základní principy anodizace, metody používané v průmyslové praxi a v práci je také popsán technologický proces. Experimentální část je rozdělena na tři základní části. První část se věnuje anodické oxidaci hliníkové slitiny AA1050. Druhá část je zaměřena na anodizaci čistého hořčíku a poslední část je zaměřena na anodizaci zinkové slitiny ZnTi2, která není tak známá jako anodizace hliníku.

Klíčová slova

Povrchová úprava, anodizace, hliník, hořčík, zinek, mikrostruktura, tvrdost, opotřebení

Bibliographic citation

REMEŠOVÁ, Michaela. *Research and development of a technology of hard anodization of nonferrous alloys.* Brno, 2020. Available online: https://www.vutbr.cz/studenti/zav-prace/detail/128704. Short version of doctoral thesis. Vysoké učení technické v Brně, Středoevropský technologický institut VUT, Central European Institute of Technology BUT. Supervisor Jozef Kaiser.

Statement

I declare that this doctoral thesis was performed independently under the supervision of Prof. Ing. Jozef Kaiser, Ph.D. and Assoc. Prof. Ing. Ladislav Čelko, Ph.D., and it is original work with using the cited sources, literature and other professional sources which are listed in the text and reference list.

In Brno, 3.7.2020 Ing. Michaela Remešová

Acknowledgement

I would like to thank the following people, without whom this thesis would not have been possible.
Thank you, supervisor Prof. Ing. Jozef Kaiser, Ph.D. for supervising this thesis. Thanks to my co-supervisor Assoc. Prof. Ladislav Čelko, Ph.D. for guidance, advice and a lot of patience. Furthermore, I would like to thank my colleagues from the research group Advanced Coatings at CEITEC BUT, namely Ivča, Melita, Vendy, Lucka, Serhii and Mirka.
Also, I would like to thank my family, especially Honza, for his patience, encouragement and support.

Thank you, CzechNanoLab Research Infrastructure supported by MEYS CR (LM2018110) for providing access to devices used for this thesis.

The part of the research has been co-financed by CEITEC BUT (the project no. STI-J-17-4623).

Contents

1. Introduction

Aluminium (Al), magnesium (Mg), zinc (Zn) and their alloys are used mainly in the automotive, aerospace, marine, and consumer industries, especially in fields where the weight reduction is critical, or where there are additional technical requirements for lightweight components. A disadvantage of these materials is related to the not very suitable surface properties such as corrosion resistance and surface hardness, which hinder their widespread use. For example, Mg and its alloys have poor corrosion resistance in most environments and require surface treatment or coating. Light metals such as those listed above are characterized by poor tribological properties, including low abrasion resistance and low strength. On the other hand, there has been a recent increase in the demand for non-ferrous metal components operating in extreme conditions (the influence of UV radiation, low/high temperature, and corrosive environments) together with higher requirements for improvement in their surface properties. One possibility to improve the aforementioned properties of these materials while increasing the service life of components is surface treatment [1-4].

A variety of surface treatment processes are being used to protect non-ferrous metals, including surface conversion treatment (e.g. chromating, phosphating), anodizing, and galvanizing/plating. These processes can be used alone or in combination with the application of organic coatings. In addition, further methods have been reported such as chemical vapour deposition (CVD), physical vapour deposition (PVD), plasma spraying and electron/laser beam surface treatments [2], which can act similarly. The anodizing technique was developed a long time ago, mainly with the aim to produce decorative coatings on Al and its alloys surfaces. Anodizing is one of the most popular industrial processes, which applies an anodic current or voltage to a substrate metal to produce a decorative, durable, corrosion-resistant, anodic coating [1, 2]. These anodic coatings are most commonly applied to protect Al, Mg, Ti and their alloys and less often to protect Zn and its alloys. Anodic coatings may be used to improve paint adhesion, strength, and chemical, mechanical and tribological properties of the metal, as a surface treatment before dyeing or as a passivation treatment. It is a very cost-effective method for producing a uniform and highly adhesive oxide/hydroxide coatings on metals. Two types of coatings can be produced: (i) compact barrier coating and (ii) porous coating [4-7]. The technological process includes (1) mechanical pre-treatment, (2) chemical pre-treatment (degreasing, etching, activation), (3) anodizing using direct current (DC), alternating current (AC) or pulse current (PC), (4) dyeing or post-treatment, and (5) sealing. Every stage has an influence on the final properties of coatings.

Several methods for anodizing of aluminium are used in the industry. Chromic acid anodizing (CAA, Type I) is used in aerospace, sulfuric acid anodizing (SAA, Type II) or decorative anodizing is used in architecture or for anodizing of subjects of daily necessity while hard anodizing (HA, Type III) is used in the mechanical engineering [8]. For industrial anodization of Mg and its alloys, the following three methods are most frequently used: Dow 9, Dow 17 and HAE. The least-used anodizing technology in the industry is anodizing of zinc. With the increasing demands on the coating properties, Al and Mg micro-arc oxidation technologies are being developed and improved [7, 9].

Most of the commercial methods require expensive processes (e.g. high temperature of the electrolyte, high voltage, etc.) or the use of hazardous/toxic chemicals (e.g. hexavalent chromium). Therefore, new and more environmentally friendly methods are being developed.

Anodically produced coatings are widely used in the automotive, aerospace, engineering and marine industries, but recently they have also been used in medicine, electrical engineering, and nanotechnology [2].

The non-uniform growth of an anodic coating is strongly influenced by the type of alloying elements or the resulting intermetallic phase and has a considerable effect on the resulting corrosion resistance, mechanical properties, and appearance of the produced coatings.

The thesis is divided into two main parts. The first part is the theoretical part and is not included in this doctoral thesis summary. The second part is the experimental part, which is focused on the optimization of the technological process of anodizing of aluminium alloy (AA1050), pure magnesium (99.9% Mg) and zinc alloy (ZnTi2). The effect of pre-treatment and anodizing conditions (concentration, composition and temperature of the electrolyte, current density/voltage, anodizing time, etc.) on the morphology, thickness, etc. of the produced anodic coatings were investigated. To improve the hardness and tribological properties of the produced anodic coatings, aluminium oxide (Al_2O_3) and polytetrafluoroethylene (PTFE) particles were added to the electrolyte.

2. Aims of the thesis

The thesis is focused on (i) the development of technological process conditions for 99.5% aluminium alloy (AA1050), zinc alloy (ZnTi2) and pure magnesium (99.9% Mg) substrates, and (ii) the characterization and evaluation of the produced anodic coatings. The main aim is focused on the production of anodic coatings doped with particles, namely aluminium oxide (Al_2O_3) and polytetrafluoroethylene (PTFE) particles, in order to improve the hardness and tribological properties of the anodic coatings when compared to the substrate. The partial aims of this work are the following:

- Optimization of (i) the mechanical and chemical pre-treatment of the substrates prior to the anodizing process and (ii) anodizing conditions in terms of temperature, concentration and type of electrolyte, current density/voltage and anodizing time.
- Detailed characterization of the produced anodic coatings via SEM with EDX, TEM, XRD, and Vickers hardness test as well as the measurement of the thickness of the anodic coatings.
- Evaluation of the effect of the anodizing process conditions on the formation and properties of the anodic coatings.
- Preparation of stable electrolytes which contain Al_2O_3 and Al_2O_3/PTFE particles in order to utilize them for the production of composite anodic coatings.
- Characterization of produced composite anodic coatings via SEM with EDX, Vickers hardness test and measurement of their thickness.
- Evaluation of the effect of Al_2O_3 and Al_2O_3/PTFE particles on the anodizing process and properties of composite anodic coatings.
- Evaluation of the effect of Al_2O_3 and PTFE particles on tribological properties of the anodic oxide coatings produced on aluminium alloys.

3. Experimental part

3.1. Experimental apparatus

Experiments were performed on the galvanic apparatus developed for this purpose. This device was equipped with ten tanks. The first three tanks were used for the chemical pre-treatment (degreasing, etching, neutralizing), and the fourth was used for the anodizing process. The rest of the tanks were used for rinsing. The anodizing tank was equipped with an external cooling system (EuroCold, Italy), a thermocouple and the direct current (DC) power supply unit QPX 1200 (Aim-TTi, United Kingdom) operating between 0-60 V and 0-50 A.

3.2. Materials and mechanical pre-treatment

3.2.1. Aluminium alloy - AA1050

A commercially pure aluminium alloy sheet (Vy-Tech, Czech Republic, AA1050) was cut into 80 mm × 60 mm × 6 mm samples which were used as the working electrodes (anodes). Two series of the samples with different mechanical pre-treatment were prepared. The first series of samples was ground and the second one was ground and further mechanically polished. The samples were masked with a polyester "acid-resistant" tape, so the resulting working electrode size was 50 mm × 60 mm × 6 mm.

3.2.2. Pure magnesium - 99.9% Mg

A commercially cold extruded pure Mg rod (12.7 mm in diameter, MG007924, Goodfellow, United Kingdom, 99.9% Mg) was cut into cylinders of 80 mm in length and then cut in half along the axis. Two series of the samples with different mechanical pre-treatment were prepared. The first series of samples was ground, and the second series of samples was ground polished. The samples surface was masked with a polyester "acid-resistant" tape to obtain the resulting working electrode area 0.19 dm^2.

3.2.3. Zinc alloy - ZnTi2

A commercially rolled ZnTi2 sheet (AlmioPlus s.r.o., Czech Republic, ZnTi2) was cut into 86 mm × 18 mm × 1 mm samples, masked with a polyester "acid-resistant" tape and used as the working electrodes (anodes) in the experiments. The resulting working electrode size was 56 mm × 18 mm × 1 mm. The chemical composition of the zinc alloy, according to the supplier, was 2% Ti and 98% Zn (wt.%).

3.3. Chemical pre-treatment

Prior to the anodizing process, all samples were chemically pre-treated, and the chemicals used were mostly of analytical grade.

3.3.1. Aluminium alloy - AA1050

First, the samples were ultrasonically degreased in acetone (min. 99.5%, p.a., Penta), ethanol (96%, p.a., Lach-Ner) and isopropyl alcohol (min. 99.7%, p.a., Lach-Ner) for 120 s in each solution. In the second step, alkaline etching in 10% NaOH (min. 98%, p.a., Lach-Ner) solution at 35 ^{o}C for 30 s was used. Subsequently, all samples were neutralized in 1:1 mixture of concentrated HNO_3 (min. 65%, p.a., Lach-Ner) and deionized water at room temperature for 60 s. After the alkaline etching and neutralizing steps, all samples were rinsed two times in deionized water, in separate tanks.

3.3.2. Pure magnesium - 99.9% Mg

First, the samples were degreased in ethanol and isopropyl alcohol in an ultrasonic bath for 120 s in each solution. In the second pre-treatment step, the samples were etched in 0.5% HF (min. 38%, p.a., Lach-Ner) for 30 s. Finally, the samples were rinsed two times in ethanol and dried with cold air.

3.3.3. Zinc alloy - ZnTi2

The samples were degreased in ethanol and isopropyl alcohol in an ultrasonic bath for 120 s in each solution, etched in 0.25% HNO_3 (65%, p.a., Lach-Ner) for 6 s, rinsed two times in deionized water and dried with cold air.

3.4. Anodizing process

3.4.1. Preparation of a stable electrolyte containing Al_2O_3/PTFE particles

Based on the available data in the literature [10-12] an anionic surfactant (98.5%, sodium dodecylbenzenesulfonate, SDBS, Sigma Aldrich) was chosen for the preparation of a stable electrolyte for further experiments. After the anodizing process under the same conditions, only Al_2O_3 particles were observed by SEM, while EDX analyses confirmed their presence on the surface of the anodic coating. Due to the PTFE particles sedimentation on the bottom of the anodizing tank, the PTFE particles were replaced with a commercial PTFE suspension for the next experiments [10]. A detailed description of the procedure with the individual stable electrolytes with PTFE and/or Al_2O_3 particles is provided in individual subchapters. The preparation of a stable electrolyte containing the particles was based on the conclusions

reported by Chen et al. [10] and Li et al. [12]. Electrolytes containing the particles were stable for more than five hours after the solution preparation.

3.4.2. Anodizing of AA1050

The anodizing process was performed in the 15% H_2SO_4 (98%, p.a., Lach-Ner) electrolyte with or without varying the composition (by adding oxalic acid ($C_2H_2O_4$, 99%, p.a., Lach-Ner) and Al_2O_3 and PTFE particles) at temperatures of (i) 24 °C, (ii) 18 °C or (iii) 10 °C under a constant voltage (16-20 V) or constant current density (1-3 A/dm^2). In all experiments, where a lower electrolyte temperature of 10 °C was used, glycerol ($C_3H_8O_3$) was added to the electrolyte to reduce the heat produced during the reactions at the oxide-substrate interface and to keep the process temperature constant. Anodizing was performed using DC power supply with two stainless steel plates, which were used as cathodes. After the anodizing process, the samples were rinsed in deionized water and dried with cold air.

The stable dispersion electrolyte solution was prepared following the protocol below:

- Solution 1: 0.6 g/L of sodium dodecylbenzenesulfonate ($CH_3(CH_2)_{11}C_6H_4SO_3Na$, 98.5%, SDBS, Sigma Aldrich) was added to 5 mL of deionized water and stirred for 30 min;
- Solution 2: 6 g/L of Al_2O_3 particles (diameter < 500 nm) were added to Solution 1, and the dispersion was stirred for 60 min in an ultrasonic bath;
- Solution 3: Solution 2 was subsequently added to 1000 mL of 15% H_2SO_4 containing 20 g/L $C_2H_2O_4$ and 10 mL/L $C_3H_8O_3$, and stirred for 30 min;
- Final electrolyte: 15 mL/L of 60 wt.% PTFE (Sigma Aldrich), a commercially available suspension, was added to Solution 3 and kept under stirring for 12 hours.

3.4.3. Anodizing of 99.9% Mg

The anodizing process was performed in the 1 M NaOH (min. 98%, p.a., Lach-Ner) electrolyte with or without Al_2O_3 and PTFE particles at 24 °C under a constant voltage of 4-50 V using DC power supply. Two stainless steel plates were used as the cathodes in the experiment. During the anodizing process, current density *vs* anodizing time was recorded at 1 s intervals, and the electrolyte was agitated with compressed air. After the anodizing process, the samples were rinsed in ethanol and dried with cold air.

The stable dispersion electrolyte solution was prepared following the protocol below:

- Solution 1: 0.6 g/L of sodium dodecylbenzenesulfonate ($CH_3(CH_2)_{11}C_6H_4SO_3Na$, 98.5%, SDBS, Sigma Aldrich) was added to 5 mL of deionized water and stirred for 30 min;
- Solution 2: 10 g/L of Al_2O_3 particles (diameter < 500 nm) were added to Solution 1, and the dispersion was stirred for 60 min in an ultrasonic bath;
- Solution 3: Solution 2 was subsequently added to 1000 mL 1 M NaOH and stirred for 30 min;

- Final electrolyte: 15 mL/L of 60 wt.% PTFE, a commercially available suspension, was added to Solution 3 and kept under stirring for 12 hours.

3.4.4. Anodizing of ZnTi2

The anodizing process was carried out under varying concentration of individual electrolytes (i) NaOH (min. 98%, p.a., Lach-Ner), (ii) KOH (min. 85%, p.a., Lach-Ner) and (iii) $C_2H_2O_4$ (99%, p.a., Lach-Ner). Also, the stable 0.5 M NaOH electrolyte solution containing 6 g/L Al_2O_3 particles was produced. Anodizing was carried out at 21 ^oC. The ZnTi2 samples and two stainless steel plates were used as the anode and the cathode in the experiment, respectively. After the anodizing process, the samples were rinsed in deionized water and dried with cold air.

The stable dispersion electrolyte solution was prepared following the protocol below:

- Solution 1: 0.6 g/L of sodium dodecylbenzenesulfonate (98.5%, SDBS, Sigma Aldrich) was added to 5 mL of deionized water and stirred for 30 min;
- Solution 2: 6 g/L of Al_2O_3 particles (diameter < 500 nm) were added to Solution 1, and the dispersion was stirred for 60 min in an ultrasonic bath;
- Final electrolyte: Solution 2 was subsequently added to 1000 mL 0.5 M NaOH and stirred for 12 hours.

3.5. Characterization techniques

X-Ray diffraction

The phase composition was identified by means of X-ray diffraction (XRD, SmartLab 3 kW, Rigaku, Japan) using Cu Kα radiation. The assessment of the peaks was performed utilizing the software HighScore Plus (PANalytical).

Scanning electron microscopy

The surface morphology and cross-section of the produced anodic coatings were investigated by SEM Lyra3 (Tescan, Czech Republic) equipped with energy-dispersive X-ray spectroscopy (EDX, XFlash 5010, Bruker AXS Microanalysis, Germany) for area/point chemical analyses.

Samples for cross-sectional microstructural observation were produced using the cold mounting technique followed by conventional metallographic procedures. As-coated cross-sectional samples were observed using the BSE mode. The metallographic preparation of ZnO samples using different mounting techniques was investigated in detail and published by the author of the thesis in Scientific Reports [13].

Transmission electron microscopy

High-resolution transmission electron microscopy (HRTEM, FEI Titan Themis 60-300, ThermoFisher Scientific, Netherlands) was used for the detailed analysis of the produced anodic ZnO coatings. TEM lamellas were prepared by focused ion beam and field emission scanning electron microscope (FIB-FESEM, FEI Helios NanoLab 660, ThermoFisher Scientific, Czech Republic).

Hardness of anodic coatings

The microhardness of non-treated AA1050 substrate and porous anodic oxide coatings was measured on cross-sectional samples using the Vickers hardness tester Duramin 100 (Struers, Denmark). The reported hardness values data are the average value of 10 individual measurements.

Ball-on-disc wear test

The tribological behaviour of the anodic coatings produced on AA1050 was evaluated using the reciprocal ball-on-disc wear test using a standard UMT TriboLab (Bruker Corporation, USA) tribometer at room temperature. The wear test counterparts (AISI G133 alumina balls, 6 mm in diameter) were stationary fixed in the holder and pressed to the moving anodized sample by a normal load of 3 N. The sample was moving back-and-forth along a stroke of 10 mm with a frequency of 3 Hz. The duration of each test was 2000 cycles. After the test, the cross-sectional profiles of wear tracks were measured using a Contour GT X8 (Bruker Corporation, USA) optical profiler, and the total wear loss of the samples was calculated as a resulting cross-sectional area of the wear track multiplied by its length.

4. Results and discussion

4.1. Anodizing of AA1050 sheet

Prior to the anodizing process, samples were mechanically and chemically pre-treated, and the effect of the pre-treatment was studied. The effects of mechanical pre-treatment and anodizing conditions on the quality and properties (morphology, thickness, hardness, etc.) of the produced anodic aluminium oxide (AAO) coatings were systematically studied. This experimental part was aimed at designing and optimising the process conditions of anodizing AA1050 and at the producing a homogenous porous anodic aluminium oxide (PAAO) coating doped with Al_2O_3 and PTFE particles of better mechanical and tribological properties when compared to the substrate.

4.1.1. Effect of pre-treatment on surface morphology

The initial substrate surface was relatively smooth with apparent scratches and rolling lines. The mechanically ground samples consisted of rough, parallel lines oriented in one direction. The surface of the polished samples was nearly smooth and contained only a small number of scratches, which were produced during mechanical polishing. Tiny featureless white spots, which indicate the presence of intermetallic phase particles, were also observed on the surface of the initial material [14-16]. Specifically, two types of intermetallic phase particles were observed: (i) irregular-shaped and (ii) round-shaped particles. An EDX analysis revealed that intermetallic phase particles present in AA1050 were most often based on binary Al-Fe or ternary Al-Fe-Si phases. After the chemical pre-treatment, the intermetallic phase particles were more visible with scalloped surface appearance, because of the lower rate of its dissolution within the aluminium matrix in the NaOH solution [17].

4.1.2. Effect of mechanical pre-treatment, voltage and current density on anodizing at 24 °C

The conditions under which the first set-up of experiments was carried out are summarized in Table 1, where the effect of pre-treatment, voltage and current density on the morphology, thickness and Vickers microhardness of the produced PAAO coatings were studied.

Table 1 *Conditions for experimental set-up to study the effect of mechanical pre-treatment, anodizing voltage and current density.*

Sample	Mechanical pre-treatment	Electrolyte (% H_2SO_4[x])	Bath temperature (°C)	Voltage (V)	Current density (A/dm^2)	Anodizing time (s)
Al 1	as-received	15	24	16	-	1800
Al 2	as-received	15	24	17	-	1800
Al 3	as-received	15	24	18	-	1800
Al 4	as-received	15	24	20	-	1800
Al 5	as-received	15	24	-	3	1800
Al 6	grinding #1200	15	24	-	3	1800
Al 7	polishing	15	24	-	3	1800

[x] H_2SO_4 - sulfuric acid

Effect of voltage/current density and pre-treatment on the morphology, thickness, and hardness of the produced porous AAO coating at 24 °C

Constant voltage - AA1050 sheet

The surface morphology of produced PAAO coatings at different voltages was almost similar in appearance to each other, but with different pore diameters. The pore diameter of PAAO coatings produced at the lowest voltage of 16 V and the highest voltage of 20 V was larger compared to the pore diameter of PAAO coatings produced at 17 and 18 V. The formed PAAO coatings copied the topography of the initial substrate state. The morphology of porous structure was more homogenous in areas where the initial surface was smoother before the anodizing process. In the cross-section, an irregular pore structure was found. The most regular porous structure could be achieved by mechanical polishing or electropolishing pre-treatment of the initial substrate and two-step anodizing process [18].

As can be seen in Fig. 1 and in Table 2, when the lowest voltage of 16 V was applied, a thicker PAAO coating of 29.5 μm was formed compared to the higher voltages of 17 and 18 V, in which the thickness of PAAO coating was 21.5 and 13.2 μm, respectively. When 20 V was applied, and almost three times shorter anodizing time was used, the thicker PAAO coating (19.5 μm) was formed. In the PAAO coating cross-section, partially oxidized intermetallic particles were found (Fig. 1a,b). The EDX analysis of PAAO coatings confirmed the presence of Al, O and S (Table 2). The presence of sulfur in the PAAO coating is the result of the incorporation of sulfur ions from the sulfuric acid electrolyte into the formed

PAAO coating during the anodizing process. As has been reported [19, 20], the negatively charged ions (i.e. O^{2-}, OH^- and SO_4^{2-}) of the electrolyte are attracted to the positively polarized anode (experimental material AA1050). On the surface of the anodized material, these ions interact with Al^{3+} cations and form the PAAO coating. The PAAO coating produced at 20 V contained more sulfur compared to PAAO coatings produced at lower voltages (see Table 2). This result indicates that using higher voltage leads to higher ionic mobility of sulfur during the anodizing process, i.e. more sulfur ions are incorporated into the formed coatings.

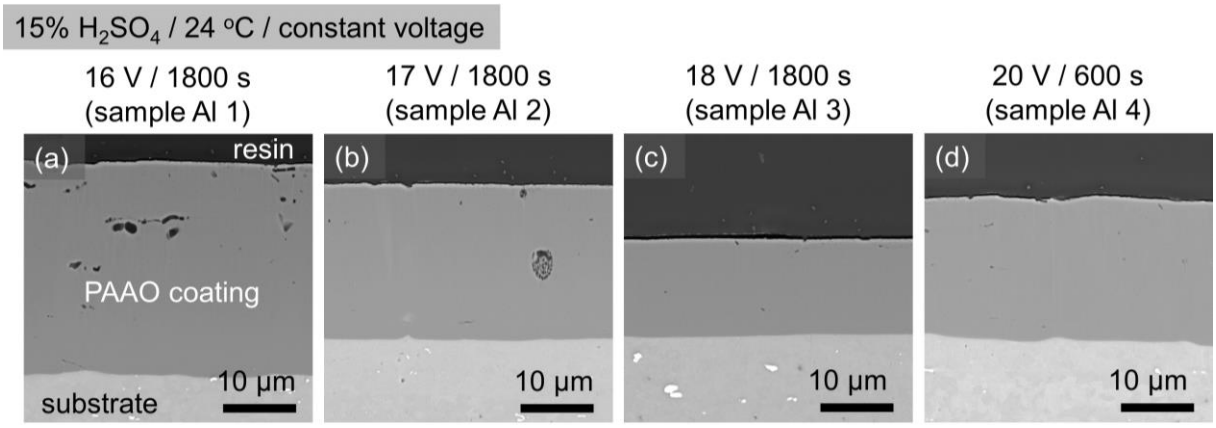

Fig. 1 *Micrographs (SEM-BSE) of the cross-section of AA1050 after anodizing in the 15% H_2SO_4 at 24 °C and at different voltages and times: (a) 16 V, 1800 s, (b) 17 V, 1800 s, (c) 18 V, 1800 s, and (d) 20 V, 600 s.*

Constant current density - AA1050 sheet

Figure 2 shows the effect of mechanical pre-treatment on the morphology and thickness of the produced PAAO coatings in the 15% H_2SO_4 at 24 °C and at a constant current density of 3 A/dm^2. On the surface of the Al 7 coating produced on a mechanically polished substrate, some cavities were found (see Fig. 2g) whose shape and dimension were similar to the intermetallic particles observed on the chemically pre-treated initial surface. These cavities were also found on the Al 6 and Al 5 PAAO coating surfaces, but in this case, the cavities were not as clearly recognized as on the Al 7 coating produced on the mechanically polished substrate. The presence of cavities on the surface can be explained by the preferred dissolution of intermetallic phase particles during the anodizing process, as observed by other authors [15, 21]. Intermetallic phase particles based on Al-Fe and Al-Fe-Si are of lower oxidation rates than the aluminium matrix, and therefore they can be trapped in the coating during the anodizing process and thus reduce the local growth of the PAAO coating [22]. After anodizing, the sample Al 5 was of a lower PAAO coating thickness (28.5 µm) than the mechanically pre-treated sample Al 6 or Al 7 (30.7 or 30.4 µm). As apparent, the grinding pre-treatment of the initial substrate surface had a negative effect on the decrease in coating microhardness, see Table 2.

Table 2 *EDX analysis of the initial substrate surface and PAAO coatings estimated from an area of 0.21 mm^2, and the thickness and microhardness of PAAO coatings.*

Sample	Element (wt.%)			Thickness of PAAO coating (µm)	Microhardness HV0.05
	Al	O	S		
Substrate	97.5	2.5	-	-	40.2±0.2
Al 1	50.0	44.6	5.4	29.5	402±9.8
Al 2	50.8	44.0	5.2	21.5	-
Al 3	50.9	43.8	5.3	13.2	-
Al 4	51.3	43.0	5.7	19.5	-
Al 5	50.2	43.8	6.0	28.5	407±8.1
Al 6	49.8	44.4	5.8	30.7	398±9.6
Al 7	50.2	44.1	5.7	30.4	405±6.3

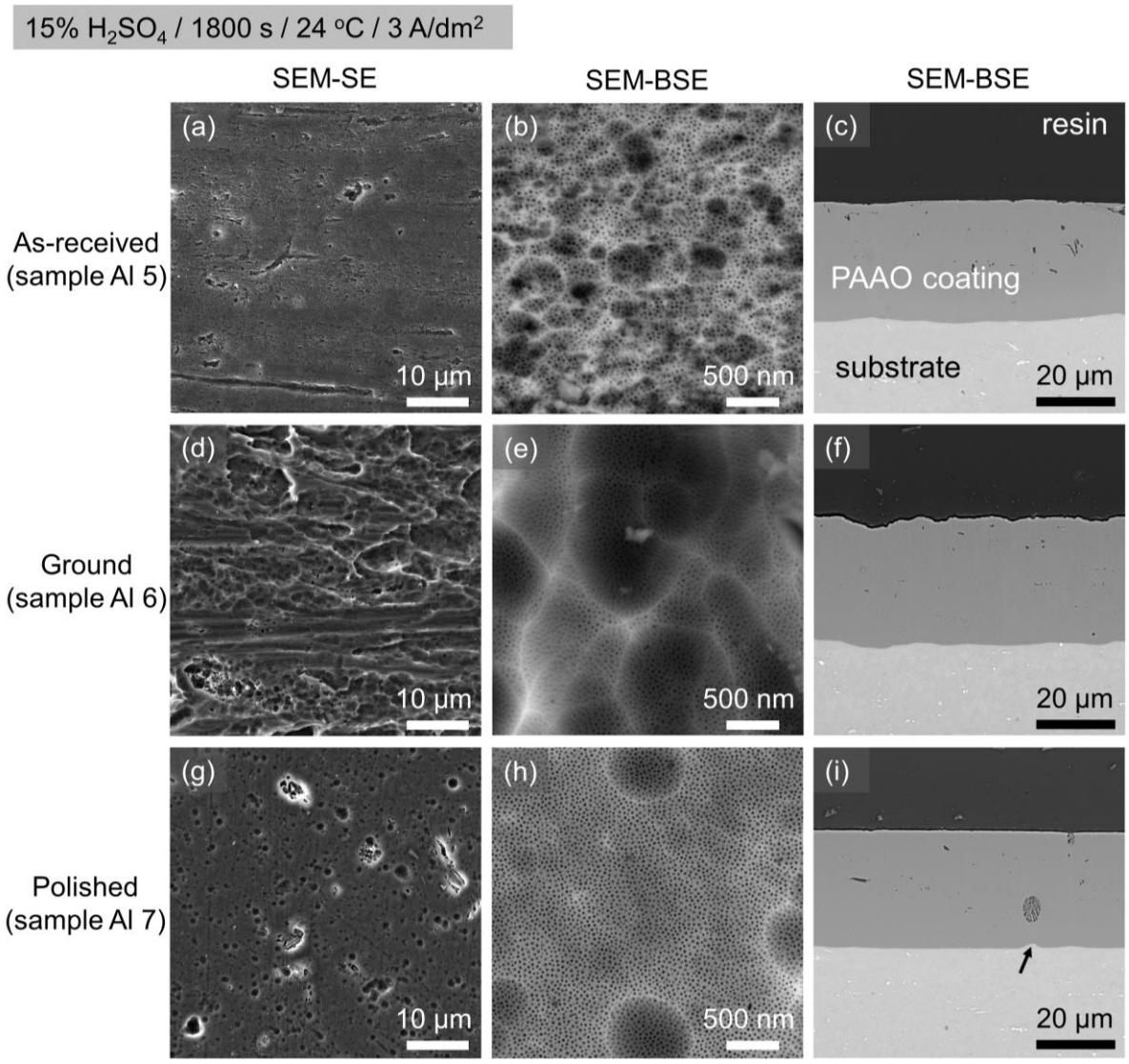

Fig. 2 *Micrographs of the coating surface (left and middle) and its cross-section (right) after the mechanical pre-treatment (a-c) as-received state, (d-f) ground, (g-i) polished and anodized in the 15% H_2SO_4 for 1800 s at 24 °C and 3 A/dm^2.*

4.1.3. Effect of temperature on the produced PAAO coating

For this experimental set-up, the temperature of the electrolyte was reduced and kept constant at 18 °C (sample Al 10) and then at 10 °C (sample Al 11). Before the anodizing process samples were polished, and then anodized in 15% H_2SO_4 at 3 A/dm^2 and for 1800 s.

Decreasing the electrolyte temperature from 24 °C to 18 °C had no significant effect on the hardness and thickness of the produced coating as in the case of lowering the temperature to 10 °C. Decreasing the electrolyte temperature from 18 °C to 10 °C increases the PAAO coating (i) thickness from 29.8 to 33.5 μm, and (ii) hardness from 417 to 451 HV0.05. A higher temperature of the electrolyte caused a higher dissolution of PAAO coating, which means that the rate of dissolution is faster than the rate of PAAO coating formation. Most scientists [7, 23, 24] studied the influence of electrolyte temperature on the thickness, porosity and hardness of the produced PAAO coatings.

On the surface and in the cross-section of the coating Al 11, produced at a lower temperature, hillocks were found. The formation of hillocks during the anodizing process of aluminium and its alloys in the sulfuric acid electrolyte was also observed by other research groups [14, 25, 26]. Hillocks indicate a local burning during the anodizing process, and this local phenomenon was observed under different anodizing conditions [27]. Generally, the local burning is caused by very high local current densities, which lead to a significant increase in the local temperature. But an exact connection between the generated heat and the origin of the hillocks is still unknown [26]. Michalska-Domanska et al. [19] observed hillocks on the surface of PAAO coatings formed on both low and high purity aluminium substrates. They proposed that the formation of hillocks is caused by the incorporation of sulfate ions rather than by the presence of intermetallic phase impurities present in anodized aluminium alloys. Detailed SEM and EDX investigations confirmed that the hillocks contained more sulfur and oxygen than the hillock-free PAAO coating did.

4.1.4. Effect of current density, electrolyte composition and concentration on anodizing process, morphology, hardness and thickness of the produced PAAO coating

Based on the previous experiments, the mechanical pre-treatment polishing, constant current density and electrolyte temperature of 10 °C were selected. The conditions for this experimental set-up are summarized in Table 3 11. In this subchapter the effect of sulfuric acid and oxalic acid concentration, the value of current density and the anodizing time was studied in order to understand better their influence on morphology, thickness and hardness of the produced PAAO coatings. Part of these results was published by the author of the thesis in Applied Surface Science journal [28].

Table 3 *Experimental conditions for the evaluation of the effect of current density, electrolyte composition and concentration on the anodizing process.*

Sample	Mechanical pre-treatment	Electrolyte	Temperature (°C)	Current density (A/dm^2)	Anodizing time (s)
Al 12	polishing	15% H_2SO_4[×] + 10 mL/L $C_3H_8O_3$[*]	10	3	1800
Al 13	polishing	15% H_2SO_4 + 20 g/L $C_2H_2O_4$[°] + 10 mL/L $C_3H_8O_3$	10	3	1800
Al 14	polishing	15% H_2SO_4 + 40 g/L $C_2H_2O_4$ + 10 mL/L $C_3H_8O_3$	10	3	1800
Al 15	polishing	15% H_2SO_4 + 20 g/L $C_2H_2O_4$ + 10 mL/L $C_3H_8O_3$	10	2	1800
Al 16	polishing	15% H_2SO_4 + 20 g/L $C_2H_2O_4$ + 10 mL/L $C_3H_8O_3$	10	1	1800
Al 17	polishing	15% H_2SO_4 + 20 g/L $C_2H_2O_4$ + 10 mL/L $C_3H_8O_3$	10	1	3600
Al 18	polishing	18% H_2SO_4 + 20 g/L $C_2H_2O_4$ + 10 mL/L $C_3H_8O_3$	10	3	1800
Al 19	polishing	10% H_2SO_4 + 20 g/L $C_2H_2O_4$ + 10 mL/L $C_3H_8O_3$	10	3	1800

[×] H_2SO_4 - sulfuric acid; $C_3H_8O_3$[*] - glycerol; $C_2H_2O_4$[°] - oxalic acid

Effect of anodizing conditions on the PAAO coating microstructure, thickness and hardness

Figures 3 shows the effect of different anodizing conditions such as electrolyte composition and current density on the morphology and thickness of the produced PAAO coatings at lower temperatures.

The surface morphology of PAAO coating Al 12 prepared at electrolyte temperature of 10 °C in the 15% H_2SO_4 electrolyte with 10 mL/L $C_3H_8O_3$ (glycerol) under a constant current density of 3 A/dm^2 (Fig. 3a-c) revealed the presence of some hillocks. The number of these hillocks was lower than the number of those observed on the coating Al 11, where $C_3H_8O_3$ addition was not used.

Addition of 10 mL/L of $C_3H_8O_3$ to the 15% H_2SO_4 electrolyte led to an increase in coating hardness from 451 to 472 HV0.05 and a decrease in coating thickness from 33.5 to 32.8 μm.

Addition of 20 g/L $C_2H_2O_4$ to the 15% H_2SO_4 electrolyte led to the formation of a harder (489 HV0.05) and thicker (34.4 μm) PAAO coating Al 13 with the typical surface morphology and with hillocks (Fig. 3d-f, Table 4). Some researchers [24, 29] observed the effect of oxalic acid on the decrease of coating porosity, which led to a higher hardness of the produced PAAO coatings. Guezmil et al. [24] showed that the alloying element influenced the microhardness of the PAAO coatings. The microhardness values obtained for AA1050 were higher than those obtained for AA5754. Fratila-Apachitei et al. [30] found that for anodized

multiphase cast aluminium alloys the copper and magnesium particles had a significant effect on the decrease in coating microhardness than silicon particles had. It is well known that Cu and Mg particles can cause macroscopic defects in the produced coating in the form of cavities.

Addition 40 g/L of $C_2H_2O_4$ had a negative effect, namely a lower coating thickness and hardness. Also, a higher number of hillocks were formed on the surface and in the cross-section of coating Al 14, as shown in Fig. 3g-i.

When the lower current density of 2 A/dm^2 was applied, the thinner (22.4 μm) and softer PAAO coating Al 15 with a lower number of hillocks was formed. A further decrease in current density down to 1 A/dm^2 resulted in the formation of a thinner PAAO coating Al 16 without hillocks, as depicted in Fig. 3j-l.

An important finding was that the PAAO coatings Al 12-Al 15 exhibited a high microhardness data scatter, which was due to the presence of a high number of hillocks on the coating surface. Roa et al. [31] studied in detail the mechanical properties of porous AAO coatings containing hillocks and confirmed by nanohardness measurements that the hillocks exhibited locally lower hardness due to higher porosity and the presence of cracks. Guezmil et al. [24] demonstrated that with an increase in current density in the range of 1-3 A/dm^2 at a fixed PAAO coating thickness of 30 μm led to an increase in PAAO coating microhardness.

Higher microstructural homogeneity was obtained by lowering the current density from 3 to 1 A/dm^2, which also provided a more uniform hardness distribution across the coating Al 17, see Fig. 3. With decreasing current density, the coating thickness decreased, which confirmed the lower mobility of O^{2-}, OH^-, SO_4^{2-} and Al^{3+} ions.

Increasing the concentration of the sulfuric acid from 15 (sample Al 13) up to 18% (sample Al 18) led to the formation of a thinner (32.3 μm) but also less hard coating (459 HV0.05) with fewer hillocks. On the other hand, the decreasing concentration of sulfuric acid from 15 to 10% led to the formation of a thicker (34.8 μm) and less hard (460 HV0.05) PAAO coating which consisted of a higher number of hillocks. With decreasing concentration of the electrolyte, the production of the hard coating was expected. Zhang et al. [32] studied the influence of the concentration of electrolyte on pore parameters and microhardness on the performance of PAAO coating on AA2024. The results showed that with increasing electrolyte concentration, the dissolution effect of the electrolyte on the formed PAAO coating decreased, resulting in higher coating porosity and lower microhardness. The decrease in hardness can be explained by the higher number of hillocks, which have a negative effect on hardness. The electrolyte concentration did not affect the coating thickness significantly as the current density did. These results are consistent with Chung et al. [33].

The EDX analysis pointed out the presence of aluminium, oxygen and sulfur in PAAO coatings; however, small differences were found in the chemical composition of coatings. PAAO coatings with hillocks Al 12-15 and Al 18-19 formed at higher current densities (2 and 3 A/dm^2, respectively) contained a higher amount of sulfur compared to coatings (Al 16 and Al 17) formed at a lower current density of 1 A/dm^2. The increase in sulfur content with increasing anodizing current density or voltage was also observed by other research teams [14, 19, 33]. Chung et al. [33] produced a PAAO coating without hillocks and found that with increasing current density, the sulfur content increased. Their results and the present study show that using a higher current density/voltage leads to higher ionic mobility of sulfur ions during the anodizing process, i.e. more sulfur ions are incorporated into the formed PAAO

coatings. The higher content of sulfur ions also contributes to the formation of hillocks, as was described above.

When a lower temperature of the electrolyte was used, the intermetallic phase particles on the surface were preferentially oxidized.

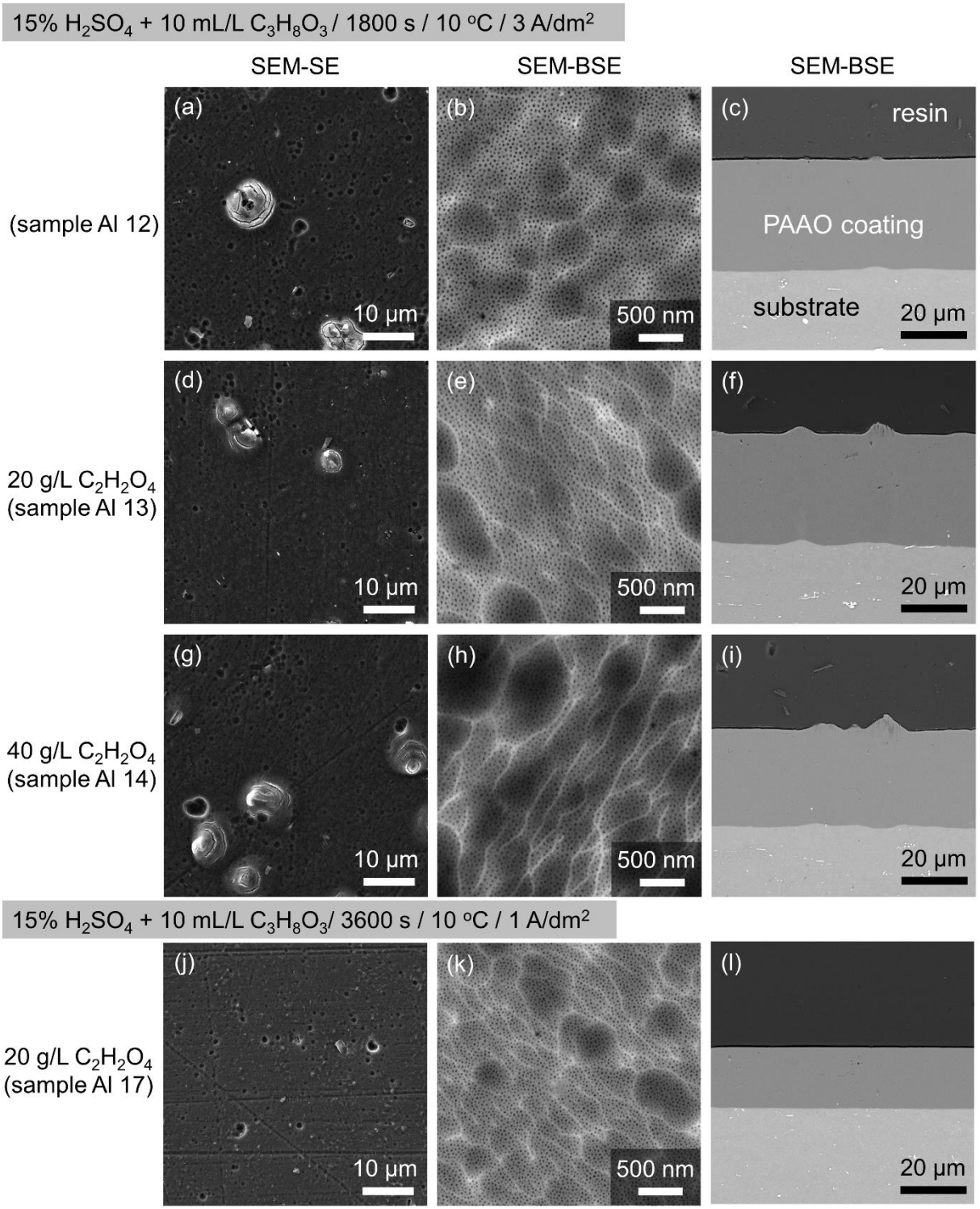

Fig. 3 *Micrographs of the coating surface (left and middle) and its cross-section (right) after anodizing: (i) at a constant current density and anodizing time (a-i) 3 A/dm², 1800 s, (j-l) 1 A/dm², 3600 s.*

4.1.5. Composite PAAO coatings containing Al_2O_3 and PTFE particles on AA1050

In this subchapter, the experiments were focused on the doping of the produced PAAO coatings by secondary particles (Al_2O_3 and PTFE) directly within the anodizing process. All detailed information about the experiment is listed in Table 4. An additional possibility of improving the mechanical and tribological properties of PAAO coatings is the development of composite anodic coatings through the addition of particles such as Al_2O_3, SiC, polytetrafluoroethylene (PTFE), and TiO_2 to the electrolyte [10, 34, 35, 36].

Table 4 *Summary of the experimental conditions for composite PAAO coating formation.*

Sample	Mechanical pre-treatment	Electrolyte	Addition of particles	Current density (A/dm^2)	Anodizing time (s)
Al 20	polishing	15% H_2SO_4 [×] + 20 g/L $C_2H_2O_4$ [°] + 10 mL/L $C_3H_8O_3$ [*]	0.6 g/L SDBS [#] + 6 g/L Al_2O_3 [£] + 15 mL/L 60 wt.% PTFE [$]	3	1800
Al 21	grinding	15% H_2SO_4 + 20 g/L $C_2H_2O_4$ + 10 mL/L $C_3H_8O_3$	0.6 g/L SDBS + 6 g/L Al_2O_3 + 15 mL/L 60 wt.% PTFE	3	1800
Al 22	polishing	15% H_2SO_4 + 20 g/L $C_2H_2O_4$ + 10 mL/L $C_3H_8O_3$	0.6 g/L SDBS + 6 g/L Al_2O_3 + 15 mL/L 60 wt.% PTFE	1	3600
Al 23	grinding	15% H_2SO_4 + 20 g/L $C_2H_2O_4$ + 10 mL/L $C_3H_8O_3$	0.6 g/L SDBS + 6 g/L Al_2O_3 + 15 mL/L 60 wt.% PTFE	1	3600

[×]H_2SO_4 - sulfuric acid; [*]$C_3H_8O_3$ - glycerol; [°]$C_2H_2O_4$ - oxalic acid; $CH_3(CH_2)_{11}C_6H_4SO_3Na$ - [#]SDBS - sodium dodecylbenzenesulfonate; [£]Al_2O_3 - aluminium oxide; [$]PTFE - polytetrafluoroethylene

Effect of Al_2O_3/PTFE particles on the PAAO coating microstructure, thickness and hardness

The chemical composition, thickness and microhardness of composite PAAO coatings are listed in Table 5. The addition of Al_2O_3 and PTFE particles makes no significant difference on the coating surface morphology. The Al_2O_3 and PTFE particles were non-uniformly distributed on the surfaces of the coatings and were in the form of agglomerates. The thickness of composite coatings (Al 20 and Al 22) was found to be thinner (24.2 and 14.1 μm) than that of the PAAO coatings (Al 13 and Al 17) without secondary particles (34.3 and 18.9 μm). This effect is related to the voltage *vs* anodizing time curve, where the voltage was found

to be lower for samples anodized in the electrolyte containing secondary particles. Moreover, composite PAAO coatings formed on the grinding pre-treated samples Al 21 and Al 23 were found to be thinner, with lower hardness and containing a higher amount of Al_2O_3 and PTFE particles on the surface, Table 5. The coating surfaces Al 20 and Al 21 produced at 3 A/dm^2 also contained hillocks. Addition of secondary particles to the sulfuric-oxalic acid-based electrolyte had a positive effect on the increasing coating hardness, as shown in Table 5. A similar effect was observed by Chen et al. [10] in that Al_2O_3 particles were entrapped in the PAAO coating and improved its hardness, while PTFE particles decreased the number and size of pore defects.

The most uniform coating morphology without hillocks and with uniform hardness distribution was achieved in the composite PAAO coating Al 22, where a combination of the polishing pre-treatment, a low anodizing current density of 1 A/dm^2 and addition of secondary particles was used for the coating formation.

Table 5 *EDX analysis of composite PAAO coatings estimated from a surface area of 0.21 mm^2, and the composite PAAO coatings thickness and microhardness.*

Sample	Element (wt.%)				Thickness of composite PAAO coating (μm)	Microhardness	
	Al	O	S	F		HV0.05	HV0.025
Al 20	50.0	43.6	5.9	0.5	24.2	512±14.3	527±14.9
Al 21	48.8	44.8	5.8	0.6	16.5	-	512±9.6
Al 22	50.5	43.9	5.2	0.4	14.1	-	521±6.3
Al 23	49.1	44.9	5.3	0.7	13.3	-	-

4.1.6. Effect of anodizing conditions on the tribological properties of anodic coatings produced on AA1050

Reciprocating sliding ball-on-disk test was used for tribological characterization of the produced anodic coatings. For tribological testing, mechanically pre-treated polished samples were selected: initial substrate, Al 7, Al 12-14, Al 17, Al 20 and Al 22. These samples were selected specifically in order to study of the effect of individual anodizing conditions (such as temperature, current density, and the additions of $C_2H_2O_4$, Al_2O_3 and PTFE particles to the electrolyte) on the coefficient of friction (COF), wear volume and wear trace depth.

Tribological testing results showed that the produced PAAO coatings had a much lower COF in comparison with the initial substrate material. No significant effect of any anodizing condition such as reducing the anodizing temperature or the addition of oxalic acid on the COF of the PAAO coatings was observed. Similarly, the addition of Al_2O_3 and PTFE particles to the sulfuric-oxalic acid-based electrolyte did not have a significant effect on changes in the COF for the anodic composite coatings Al 20 and Al 22, when compared to previous studies [10, 37].

Current density reduced from 3 to 1 A/dm^2 led to a decrease in COF in the produced coatings Al 17 and Al 22.

The decrease in the electrolyte temperature from 24 to 10 ^oC promoted the reduction in wear loss in the coating Al 12 as compared to the PAAO coating Al 7. Addition of oxalic acid to the electrolyte and reduction of the current density resulted in slightly lower wear resistance. The improvement in the wear resistance of anodic coatings by way of reducing the electrolyte temperature is in full compliance with the study of Lu et al. [38], and it is assumed that it is primarily associated with the decrease in the AAO coating porosity and in the reduction of defects such as hillocks, local cracks, etc., which enables mechanical properties of the coating. Contrary to data reported by Guezmil et al. [24], the evidence of a wear loss reduction for harder and less porous coatings with a lower number of hillocks on the surface indicates that the wear resistance of PAAO coatings may be influenced not only by the amount of porosity, surface roughness or hardness but also by other features such as shear strength and crack resistance. This conclusion was demonstrated by adding Al_2O_3 and PTFE particles to the electrolyte, which led to a significant reduction in wear loss; this loss was found to be the lowest for the composite anodic coatings Al 20 and Al 22. Despite the absence of significant effects of the particles on the COF of the PAAO coatings. It is evident that the presence of secondary particles in composite anodic coating results in improved shear strength and elasticity of the coatings, and thus the composite anodic coatings were more resistant to the deformation in the reciprocal sliding test and without any significant coating break up.

4.1.7. Closing remarks on anodizing of AA1050

Mechanical and chemical pre-treatment and wide range of anodizing conditions, including voltage, current density, electrolyte temperature and composition, and addition of Al_2O_3 and PTFE particles to the electrolyte, have been applied to AA1050 substrate to produce porous anodic aluminium oxide coatings. The main conclusions can be listed as follows:

Effect of pre-treatment on surface morphology

- Polishing is a more suitable pre-treatment technique for aluminium samples than grinding since the surface is more uniform and smooth.
- The intermetallic phase particles contained in AA1050 were based on binary Al-Fe or ternary Al-Fe-Si phases.
- AA1050 contained intermetallic phase particles of irregular-shape and round-shape. The number of round-shape particles was lower than the number of irregular-shape particles, the latter containing a higher amount of silicon.

Effect of mechanical pre-treatment, voltage/current density and temperature on the anodizing process and production of PAAO coatings

- Porous anodic aluminium oxide coatings were produced during potentiostatic anodizing at 16-20 V in 15 % H_2SO_4 at 24 ^oC.
- Porous AAO coatings were also produced during a galvanostatic anodizing process at 3 A/dm^2 in the 15 % H_2SO_4 at 24 ^oC.
- XRD results showed that the anodized coatings were composed of amorphous aluminium oxide, and EDX analysis confirmed the presence of Al, O and S.

- Reducing the electrolyte temperature from 24 to 10 °C during the galvanostatic anodizing process at 3 A/dm^2 led to increasing the voltage, and the oxidation rate was higher than the dissolution rate. A thicker and harder coating containing hillocks with local cracks was produced.
- With decreasing electrolyte temperature, the sulfur content increased in the PAAO coating, suggesting the incorporation of sulfate ions in the PAAO coating and the formation of hillocks. The hillocks contained more sulfur, and their hardness was lower than that of the surrounding PAAO coating.

Effect of current density, electrolyte composition and concentration on the anodizing process, morphology, hardness and thickness of the produced PAAO coating

- Addition of 10 ml/L glycerol to the 15% H_2SO_4 electrolyte resulted in the formation of a PAAO coating with a lower number of hillocks and increased coating hardness.
- Addition of 20 g/L of oxalic acid to the 15% H_2SO_4 electrolyte also had a possible effect on increasing the thickness and hardness of produced coatings but not such as was observed in the case of a decrease in the temperature of the electrolyte. Further addition of oxalic acid to sulfuric acid had a negative effect on coating hardness.
- The decrease in current density from 3 to 1 A/dm^2 led to a significant voltage drop, which resulted in lower mobility of O^{2-}, OH^-, SO_4^{2-} and Al^{3+} ions. By reducing the current density, a 3.5-times thinner coating without cracks and hillocks was produced at the same time.
- A stable electrolyte containing secondary particles was produced using the sodium dodecylbenzenesulfonate anionic surfactant, Al_2O_3 powder and commercial 60 wt.% PTFE suspension.
- Addition of 6 g/L Al_2O_3 and 15 mL/L 60 wt.% PTFE particles and 0.6 g/L sodium dodecylbenzenesulfonate to the sulfuric-oxalic acid-based electrolyte led to a decrease in voltage. The decrease in voltage caused lower incorporation of sulfur into the coating, and thinner and harder coatings were produced. The microstructural examination revealed successive incorporation of Al_2O_3 and PTFE particles in the produced coatings.
- The most uniform coating morphology without hillocks and with uniform distribution of hardness was achieved by the combination of the polishing pre-treatment and the low anodizing electrolyte temperature of 10 ^oC, the low anodic current density of 1 A/dm^2, and the addition of Al_2O_3 and PTFE particles to the sulfuric-oxalic acid-based electrolyte.

Effect of anodizing conditions on the tribological properties of the anodic coatings produced on AA1050

- Significant effect on wear resistance had the anodizing conditions such as lower electrolyte temperature of 10 ^oC and addition of Al_2O_3 and PTFE particles to the sulfuric-oxalic acid electrolyte. A combination of these conditions resulted in 30% higher wear resistance.
- The porous composite AAO coating without structural defects (hillocks and cracks) and with the best combination of mechanical properties was prepared by anodizing at a low temperature of 10 °C and lower current density of 1 A/dm^2 in the sulfuric-oxalic acid electrolyte with a dispersion of Al_2O_3 and PTFE particles.

4.2. Anodizing of 99.9% Mg

4.2.1. Optimization of anodizing conditions for 99.9% Mg

The formation of anodic magnesium hydroxide coatings (AMHCs) was performed in the 1 M NaOH electrolyte at 24 ^{o}C, utilizing a constant voltage in the range of 4 to 50 V. The effects of mechanical pre-treatment (grinding and polishing) of the initial substrate and voltage on the anodizing process were studied. The experimental conditions are summarized in Table 6 and were chosen based on earlier results [39].

Table 6 *Experimental conditions to study the effect of pre-treatment and utilized voltage.*

Sample	Mechanical pre-treatment	Electrolyte (C_{NaOH}[¶])	Voltage (V)	Anodizing time (s)
Mg 1	grinding (#1200)	1 M	4	1200
Mg 2	polishing (1 μm)	1 M	5	1200
Mg 3	grinding (#1200)	1 M	5	1200
Mg 4	polishing (1 μm)	1 M	10	1200
Mg 5	polishing (1 μm)	1 M	20	1200
Mg 6	grinding (#1200)	1 M	20	1200
Mg 7	polishing (1 μm)	1 M	50	1200

[¶]NaOH - sodium hydroxide

Anodizing process

Figure 4 shows the current density vs anodizing time curves obtained on 99.9% Mg during the potentiostatic anodizing process. Two different shapes of curves were recorded based on the voltage used. Salaman et al. [40] also recorded two shapes of curves (i) at a low voltage of 3 V and (ii) at a higher voltage of 10-100 V during anodizing AZ31 magnesium alloy in the 1 M NaOH electrolyte.

The first type of the anodizing curve shape appeared when lower voltage values were used, namely 4 and 5 V (curves Mg 1 and Mg 2, Mg 3, Fig. 4). The current density did not increase immediately that the voltage was applied. The current density started to increase after 5 s from the beginning of the anodizing process, and this was a result of the dissolution reaction of pure Mg surface substrate (Mg 1-Mg 3) in the electrolyte. Then, magnesium ions reacted with hydroxide ions, and an anodic coating of magnesium hydroxide ($Mg(OH)_2$) started to form. The maximum current density reached the values 3.1 A/dm^2, 9.4 A/dm^2 and 11 A/dm^2 for the curves Mg 1, Mg 2 and Mg 3 at about 40 s (Fig. 4b), respectively; after that, however, the current density grew slowly until the end of the anodizing process, which indicated the growth of the AMHC.

When a voltage of 5 V was applied, a much steeper slope of the current density was recorded (curves Mg 2 and Mg 3) compared to the 4 V (curve Mg 1). This behaviour could be caused

by the fact that the dissolution of the magnesium matrix was faster than the formation of the $Mg(OH)_2$ coating.

When higher voltages of 10, 20 and 50 V (curves Mg 4-Mg 7, Fig. 4) were used, the current density immediately increased with anodizing time, which is related to the dissolution reaction of pure Mg substrate. When the local maximum of current density was reached, the current density decreased with anodizing time, and AMHC was produced. Finally, the current density was kept constant with anodizing time due to the stationary dissolution and AMHC formation [41].

The reaction during the Mg 1-Mg 3 and Mg 7 experiments was intense, and the evolution of oxygen gas bubbles was more visible during the anodizing process compared to the Mg 4-Mg 6 experiments.

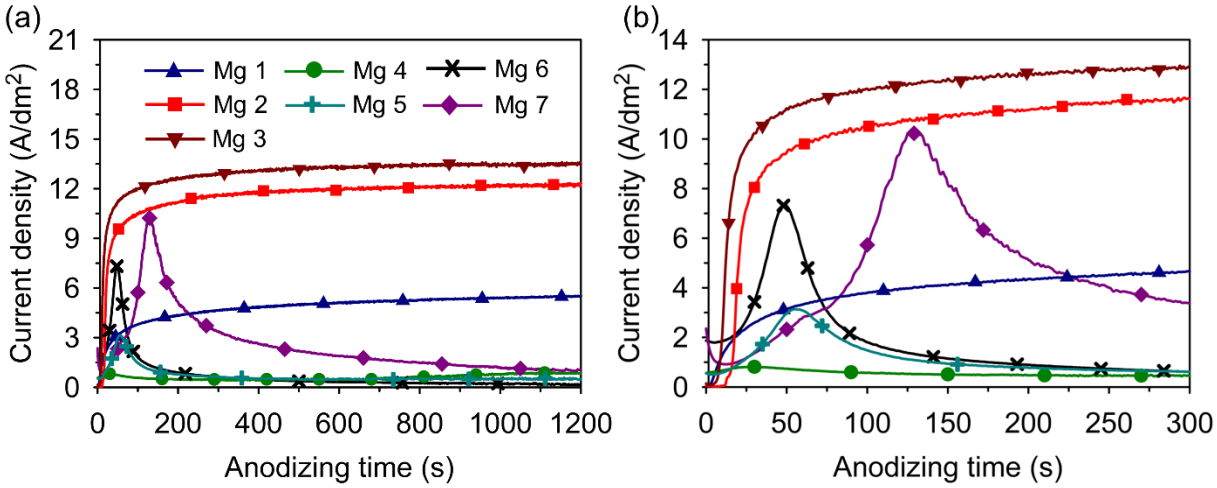

Fig. 4 *Current density vs anodizing time curves recorded during anodizing of pure magnesium in the 1 M NaOH at 24 °C for 1200 s at different voltages (a) after 1200 s, and (b) a detail of the record up to 300 s.*

Microstructure and composition of anodic coatings

Anodic magnesium hydroxide coatings (Mg 1-Mg 3) produced at a low voltage of 4 V and 5 V, respectively, were found to be of a different morphology than the coatings Mg 5-Mg 7, which were produced at higher voltages (10-50 V). The anodic magnesium hydroxide coating Mg 1 produced at 4 V was compact and denser than the coatings Mg 4-Mg 7 produced at higher voltages (10-50 V). The coating had a bulk-like structure with the rough coating surface. On the surface after anodizing, only a few microcracks were observed, while scratches from the mechanical pre-treatment were not found. The thickness of the produced anodic coating was 10.8 μm. In the cross-section, horizontal cracks were observed, and their presence can be explained by the rapid growth of the coating together with the oxygen gas evolution during the anodizing process.

When a higher voltage of 5 V was used, non-uniform coatings (Mg 2 and Mg 3) were produced. On the coating surfaces, two different areas were found, which consisted of (i) hemispherical dimples containing an increased amount of oxygen, and (ii) only a slightly anodized magnesium initial material. The AMHC was formed preferably in the dimples area, and the morphology of coatings was similar to the coating Mg 1. The presence of dimples can be explained by the local dissolution of pure magnesium matrix that initiates the formation

of separate dimples. The number of dimples increases with anodizing time, and they eventually interlink each other to form a larger area. The process continues until the magnesium surface is completely activated [42]. This mechanism was observed for coating Mg 1, and these results are in correlation in the AMHC growth theory proposed by Kim et al. [42].

When a higher voltage (10-50 V) was applied, thinner and compact anodic coatings with micropores were produced. On the surface of anodic hydroxide coatings (Mg 3 and Mg 6) scratches coming from the mechanical ground pre-treatment process were observed. With the voltage increasing from 10 to 50 V, more oxygen was detected in AMHC. In the cross-section of the coating Mg 6, a very thin AMHC was found compared to the anodic coating Mg 1 produced at 4 V.

The coatings Mg 1, Mg 2 and Mg 7 contained extra sodium compared to the coatings Mg 4-Mg 6. The presence of sodium in the coatings was the result of also incorporating sodium ions from the sodium hydroxide electrolyte into coatings during the anodizing process at 4, 5 and 50 V.

The XRD patterns indicate that the anodic coatings produced at different voltages are mainly composed of $Mg(OH)_2$ and Mg phases. The preferential formation of the $Mg(OH)_2$ phase at a lower anodizing voltage (3 V) was found instead of the MgO phase, and our results are in correlation with the published results of Kim et al. [43]. The MgO phase is preferentially formed during plasma electrolytic oxidation at higher voltages (> 80 V) [43].

4.2.2. Effect of addition of Al_2O_3 and PTFE particles on the anodizing process and morphology of the produced composite anodic coating

Based on the previous experiments, a constant voltage of 4 and 20 V was used to produce the composite anodic coating (CAC). Added to the 1 M NaOH electrolyte were 10 g/L Al_2O_3, 15 mL/L 60 wt.% PTFE and sodium dodecylbenzenesulfonate surfactant (SDBS). The experimental conditions are summarized in Table 7.

Table 7 *Summary of the experimental conditions aimed to form composite anodic coatings.*

Sample	Mechanical pre-treatment	Electrolyte (C_{NaOH}[¶])	Particles addition	Voltage (V)	Anodizing time (s)
Mg 1P	grinding (#1200)	1 M	0.6 g/L SDBS[#] + 10 g/L Al_2O_3[£] + 15 mL/L 60 wt.% PTFE[$]	4	1200
Mg 5P	polishing (1 μm)	1 M	0.6 g/L SDBS + 10 g/L Al_2O_3 + 15 mL/L 60 wt.% PTFE	20	1200
Mg 6P	grinding (#1200)	1 M	0.6 g/L SDBS + 10 g/L Al_2O_3 + 15 mL/L 60 wt.% PTFE	20	1200

[¶]NaOH - sodium hydroxide; $CH_3(CH_2)_{11}C_6H_4SO_3Na$ - [#]SDBS - sodium dodecylbenzenesulfonate; [£]Al_2O_3 - aluminium oxide; [$]PTFE - polytetrafluoroethylene

Anodizing process

Adding Al_2O_3 and PTFE particles to the 1 M NaOH electrolyte led to an increase in current density and started the dissolution process of pure Mg substrate, which is apparently based on the current density *vs* anodizing time curves, see Fig. 5. The progress of the curves was found to be the same as in the case of anodizing without additional Al_2O_3 and PTFE particles, Fig. 4.

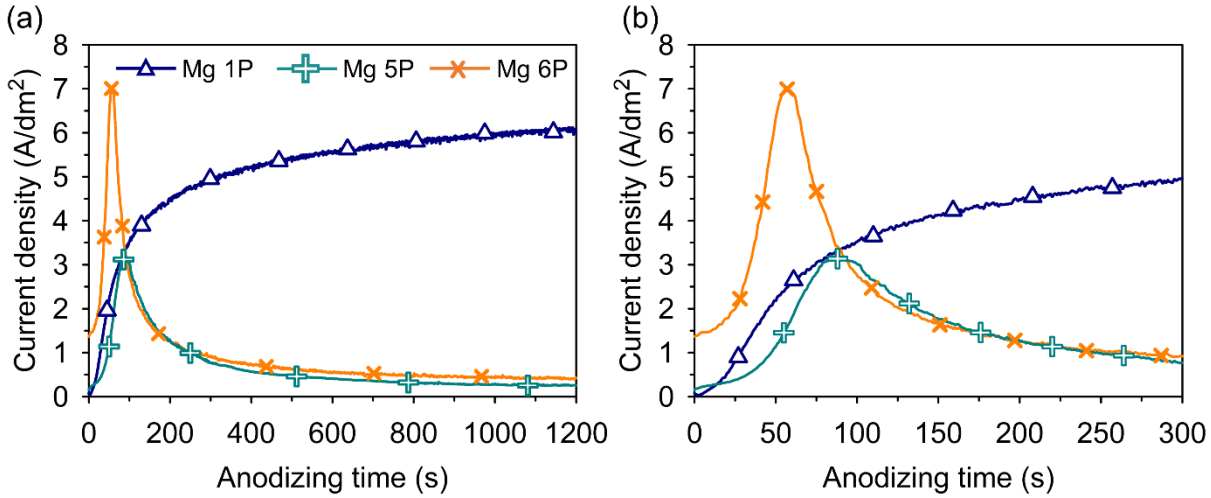

Fig. 5 *Current density vs anodizing time curves recorded during anodizing of pure Mg in the 1 M NaOH electrolyte with Al_2O_3 and PTFE particles at 24 °C for 1200 s (a) after 1200 s, and (b) a detail of the record up to 300 s.*

Microstructure and composition of anodic composite coatings

SEM and EDX results indicated that the Mg surface was rich in Al_2O_3 and PTFE particles after the anodizing process. On the free surface of the coating Mg 1P produced at 4 V, two different areas were observed: (i) hemispherical dimples with the composite anodic coating and (ii) partially oxidized magnesium matrix with Al_2O_3 and PTFE particles. The coating microstructure was found to be the same as that of Mg 2 and Mg 3 AMHCs produced at 5 V. The particles were found to be strongly incorporated in the magnesium matrix because after washing in an ultrasonic ethanol bath, the particles remained on the surface of the anodized sample. In the cross-section (i) a local composite anodic coating with horizontal cracks and (ii) a coating containing Al_2O_3 and PTFE particles were observed. Addition of Al_2O_3 and PTFE particles to the electrolyte led to an increase in current density, which resulted in the production of non-compact CAC compared to the Mg 1 coating without the addition of particles to the electrolyte. Reducing the anodizing voltage to less than 4 V (maximum anodizing current density 4 A/dm^2) could lead to the formation of compact CAC.

The surface morphology of both produced coatings without particles and with particles, exhibited some similar features. When comparing high magnification micrographs without and with Al_2O_3 and PTFE particles, a different morphology was observed. An EDX analysis of the composite anodic coating confirmed the presence of Mg, O, Na, Al and F. More Al and F was found on the Mg 6P coating surface, which was of higher roughness before anodizing. The results indicated that the added Al_2O_3 and PTFE particles were incorporated into the coating during the formation of a composite anodic coating.

In the literature, no other similar study was found that would focus on the direct incorporation of Al_2O_3 and PTFE particles from the electrolyte during the anodizing process at lower voltages ($\leq$ 50 V). Further systematic experiments are needed to understand the process of incorporating these secondary particles during the anodizing process.

4.2.3. Closing remarks on anodizing of 99.9% Mg

The effects of mechanical pre-treatment (grinding and polishing) of the initial material (pure magnesium) and anodizing conditions such as voltage and addition of Al_2O_3 and PTFE particles to the 1 M NaOH electrolyte on the formation of anodic coatings were examined. The following main conclusions can be drawn:

- Compact anodic magnesium hydroxide coatings (AMHCs) were successfully produced *via* a one-step potentiostatic anodizing process of pure magnesium in the 1 M NaOH electrolyte at 21 ^{o}C, 4 and 10-50 V.
- During the anodizing process, two different shapes of current density *vs* anodizing time curves were recorded, depending on the applied voltage. When a lower voltage of 4 or 5 V was used, the current density increased with anodizing time and more gas oxygen was observed. On the other hand, when a higher voltage was applied, the current density immediately increased and then, after reaching the maximum of current density, decreased with anodizing time.
- Using a lower voltage of 4 V, a thicker (10.8 μm), bulk-like structure coating with horizontal cracks and the rough surface was produced. Increasing the voltage to 5 V led to the formation of non-compact coating with hemispherical dimples containing AMHC with cracks and a slightly anodized magnesium substrate. Vigorous gas evolution during the anodizing process caused the formation of horizontal cracks inside the coatings. When using a higher voltage (10-50 V), a thinner (nm) and smoother coatings with micropores were produced. The coating produced at 50 V was denser, smoother and contained larger micropores, which related to the intensive oxygen gas evolution during the anodizing process.
- Addition of Al_2O_3 and PTFE particles directly to the electrolyte caused an increase in current density during the anodizing process. A non-compact composite coating was produced at 4 V due to the increase in current density. On the coating surface, three different areas were observed: (i) hemispherical dimples containing composite anodic coating, (ii) partially oxidized magnesium substrate with Al_2O_3 and PTFE particles, and (iii) Al_2O_3 and PTFE particles coating. The anodic composite coating produced at 20 V was compact, and the Al_2O_3 and PTFE particles were successively incorporated into the produced coatings. The ground anodized sample contained more Al_2O_3 and PTFE particles.

4.3. Anodizing of ZnTi2

4.3.1. Effect of voltage, NaOH electrolyte concentration and anodizing time on the resulting morphology, structure and thickness of anodic coatings

Experimental work was designed in order to evaluate the effect of voltage, concentration of the NaOH electrolyte, and anodizing time on the resulting structure, morphology, and thickness of the produced anodic coatings. Various NaOH concentrations were used further to analyse the concentration effect on the anodizing process conditions. Preferential anodizing conditions are summarized in Table 8.

Table 8 *Experimental conditions for the evaluation of the effect of the NaOH electrolyte concentration and voltage on the anodizing process of ZnTi2.*

Sample	Electrolyte (C_{NaOH}¶)	Voltage (V)	Anodizing time (s)	pH
Zn 1	0.04 M	50	900	12.6
Zn 10	0.04 M	50	1800	12.6
Zn 2	0.1 M	50	900	13.0
Zn 11	0.1 M	50	1800	13.0
Zn 12	1.0 M	4	1800	13.6
Zn 13	0.5 M	4	1800	13.4
Zn 14	0.3 M	4	1800	13.3
Zn 5	0.3 M	4	900	13.3
Zn 15	0.3 M	4	300	13.3

¶NaOH - sodium hydroxide

Characterization of the produced ZnO coatings

Effect of voltage and NaOH concentration on overall appearance, and the chemical and phase composition

Due to the anodizing process, two different types of ZnO anodic coating were formed and referred to as “black” and “white” respectively. Samples anodized in the 0.04-0.1 M NaOH electrolytes at 50 V were white in appearance. The samples anodized in the 0.3-1 M NaOH electrolytes at 4 V were found to be black colour. The voltage used influenced the appearance of the produced anodic coatings, which can also relate to the evolution of oxygen. Mabon et al. [44] proposed that black ZnO anodic coatings produced in alkaline electrolytes exhibited good solar-selective properties for application as an absorber surface for low temperature photothermal solar energy conversion. Therefore, more attention should be paid to the overall

appearance of the anodic coatings, which is closely connected to its optical properties. The influence of process conditions on the overall appearance (i.e. colour) of ZnO anodic coatings is not even discussed in the literature, and only a limited number of authors comment on the resulting appearance for a specific combination of process conditions. For example, Rocca et al. [45] observed the formation of grey ZnO anodic coatings in the 0.05 M KOH at 50 V. Zhang et al. [46] described that anodic coatings of various colours, from white through grey to black, can be produced in NaOH and Na_2CO_3 aqueous solutions in dependence on the current density. Mika et al. [47] found that the dark nanoporous ZnO coatings could be obtained in the strongly alkaline electrolyte (i.e. 1 M NaOH) at 2 and 4 V.

The XRD analysis confirmed polycrystalline ZnO with hexagonal (wurtzite) structure. The EDX analysis confirmed the presence of Zn, O and Na.

Effect of electrolyte concentration on the growth and thickness of ZnO coating

The effect of electrolyte concentration on the morphology of the ZnO coatings was investigated using (i) the 0.04 and 0.1 M NaOH electrolytes at 50 V and (ii) the 0.3, 0.5 and 1 M NaOH electrolytes at 4 V, the anodizing time was kept the same, i.e. 1800 s. The coating surface free morphology and cross-section micrographs are shown in Figs. 6 and 7, respectively.

At a high voltage of 50 V, coatings with the white appearance and similar surface morphology for both electrolyte concentrations, i.e. 0.04 and 0.1 M NaOH, were produced, see in Fig. 6. In the high magnification micrographs of the coating surface (Fig. 6a,b) the granular structure can be seen. The presence of cracks on the free surface seems to be closely related to the horizontal cracks and gaps which were observed over the thickness of the whole coating (Fig. 6c,d). Even the coating thicknesses (16.4 μm and 17.7 μm) did not significantly change with the electrolyte concentration. Nevertheless, with the increasing concentration of the NaOH electrolyte, the bulk-like structure contained a lower number of horizontal cracks and gaps were formed, see Fig. 6c,d. Longer anodizing time did not affect the morphology of produced coatings compared to coatings Zn 1 and Zn 2 produced in the shorter anodizing time,i.e. 900 s, but had an effect on the coating thickness. With the anodizing time increasing from 900 s to 1800 s, the thickness of ZnO coatings increased from 8.3 to 16.4 μm and from 11.0 to 17.7 μm respectively.

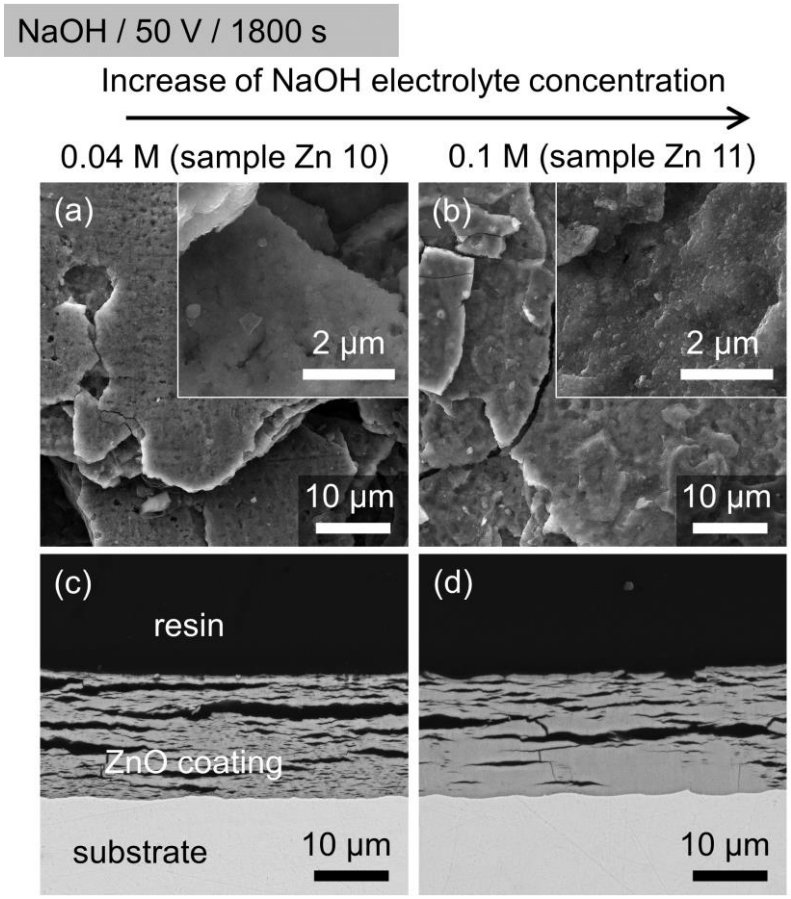

Fig. 6 *Micrographs of the (a, b) free surface (SEM-SE), and (c, d) cross-section (SEM-BSE) of ZnO coatings formed at 21 °C and at 50 V for 1800 s in the: (a, c) 0.04 M NaOH, and (b, d) 0.1 M NaOH electrolyte.*

Decreasing the voltage from 50 to 4 V led to the formation of anodic coatings that were different in structure and appearance, see Fig. 7. Anodic coatings produced at 4 V were dark black, and a sponge-like structure was produced, as can be seen in the cross-section in Fig. 7d-f. With the electrolyte concentration increasing from 0.3 to 1 M NaOH, the thickness of anodic coating increased non-linearly (2.5, 4.8 and 9.4 µm), and a coating with bulk-like structure and smaller pores was produced, as can be seen in the cross-section in Fig. 7d-f. On the other hand, the anodic coating formed in the 1 M NaOH electrolyte contained undesirable vertical microcracks, and the coating surface was smoother and had a finer granular structure. At higher electrolyte concentrations, a higher number of Zn^{2+} and OH^- ions participate in the formation of a coating, and therefore, the thicker coating can be produced. The effect of anodizing time (i.e. 300, 900 and 1800 s) during the anodizing process at 4 V in the 0.3 M NaOH was also studied. As might be expected, longer anodizing time led to the formation of thicker anodic coatings, from 2.5 to 4.8 up to 9.5 µm. Dong et al. [48] anodized pure Zn foil in the 0.1 M NaOH at 5-40 V and found that the ZnO coatings produced at lower voltages (< 9 V) were thinner, the thickness did not change with the voltage range from 5 to 9 V, and they exhibited a porous structure. ZnO coatings produced at 12 V were thicker and exhibited a nanorod structure. Dong et al. [48] explained the formation of the porous structure as the result of an insufficient supply of voltage. When the voltage was lower than 9 V, the migration of OH^- and O^{2-} ions was lower, and therefore these ions were unable to pass through the produced ZnO coating as in the case when 12 V was used. The

residual ions tend to diffuse freely and attacked the formed ZnO coating randomly. When using a higher voltage, the ions could pass through the produced ZnO coating, and a thicker and regular nanorod structure could be produced, i.e. the oxidation and dissolution rates were in balance. With the voltage increasing from 20 to 40 V, the nanorod ZnO coating became thicker and contained horizontal cracks and gaps.

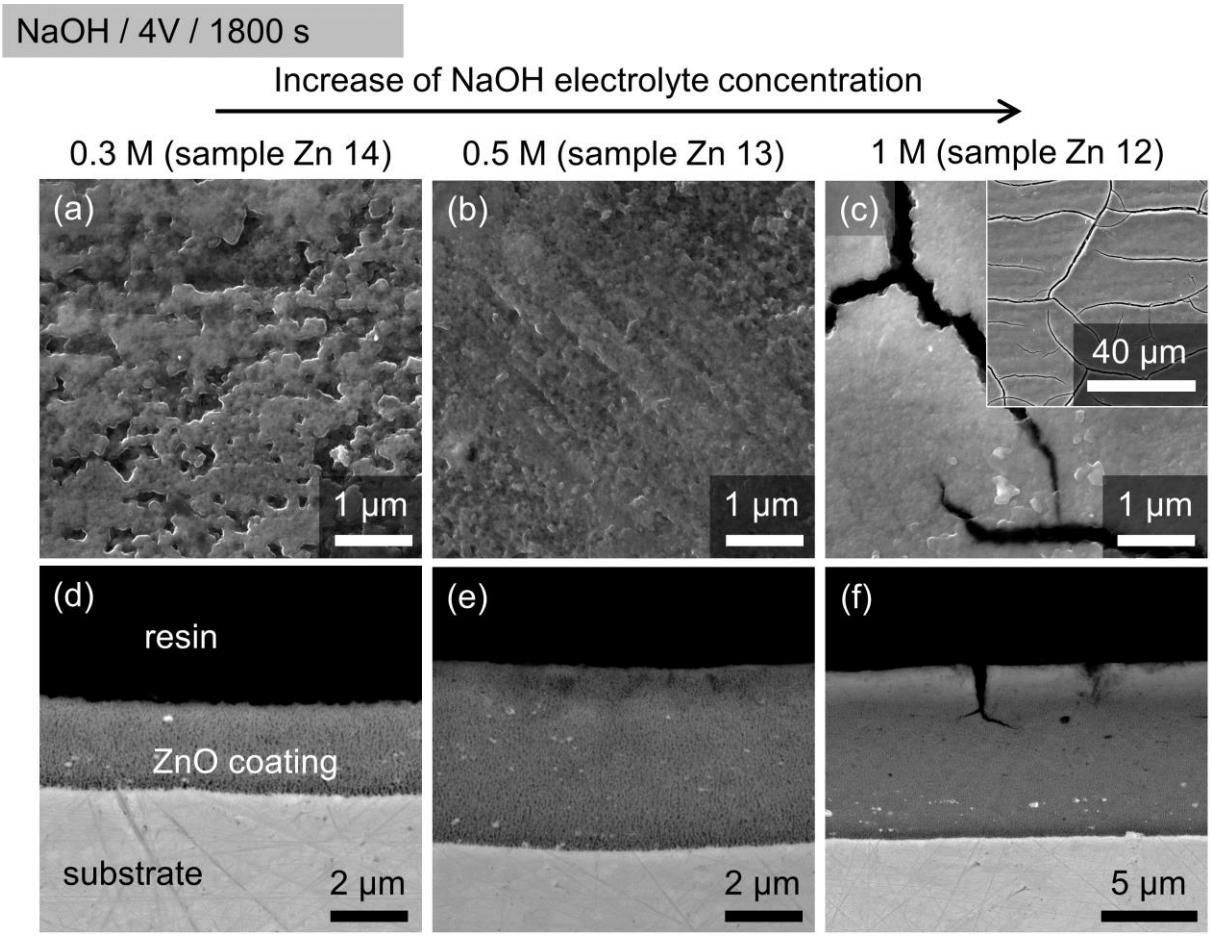

Fig. 7 *Micrographs of the (a-c) free surface (SEM-SE), and (d-f) cross-section (SEM-BSE) of ZnO coatings after anodizing at 21 °C, 4 V for 1800 s in the: (a, d) 0.3 M NaOH, (b, e) 0.5 M NaOH, and (c, f) 1 M NaOH.*

Anodic coatings Zn 11 (0.1 M NaOH, 50 V and 1800 s, “white”) and Zn 14 (0.3 M NaOH, 4 V, 1800 s, “black”) were investigated in detail by FESEM and HRTEM. The coating surface morphology of Zn 11 contained densely arranged and piled up smaller globular nanoparticles compared to the coating Zn 14.

Both ZnO coatings Zn 11 and Zn 14 consist of overlapping ZnO crystalline grains. Based on the results, it can be assumed that the coating Zn 11 produced at 50 V is made up of nanorods rather than nanotubes. The EELS spectra for both coatings were identical.

4.3.2. Composite anodic coatings containing Al_2O_3 particles on ZnTi2 alloy

The sodium hydroxide electrolyte (0.5 M) with 6 g/L Al_2O_3 particles and two types of agitation were used; (i) compressed air and (ii) magnetic stirring to produce the composite anodic coatings (voltage 4 V). The distance between the anode and the cathode was (i) 70 and (ii) 40 mm. The conditions of all experiments are summarized in Table 9.

Table 9 *Summary of the experimental conditions for composite anodic coating formation.*

Sample	Electrolyte	Temperature (°C)	Voltage (V)	Anodizing time (s)	Type of agitation
Zn 17	0.5 M NaOH[¶] + 0.6 g/L SDBS[#] + 6 g/L Al_2O_3[£]	21	4	1800	compressed air
Zn 18	0.5 M NaOH + 0.6 g/L SDBS + 6 g/L Al_2O_3	21	4	1800	magnetic stirring

[¶]NaOH - sodium hydroxide; $CH_3(CH_2)_{11}C_6H_4SO_3Na$ - [#]SDBS - sodium dodecylbenzenesulfonate; [£]Al_2O_3 - aluminium oxide

Effect of anodizing conditions on the morphology and thickness of the produced anodic composite coating

The free surfaces and cross-sections of the produced composite anodic coatings utilizing different agitation mechanisms, i.e. compressed air or magnetic stirring, are shown in Fig. 8a-c and Fig. 8d-i, respectively. On the coating surface (Fig. 8) produced with compressed air agitation, uniformly distributed and aggregated Al_2O_3 particles were observed. Addition of Al_2O_3 particles to the 0.5 M NaOH electrolyte did not affect the morphology and thickness of the produced composite anodic coatings when compared to the coating Zn 13 without Al_2O_3 particles. On the other hand, magnetic stirring affected the morphology of the produced anodic composite coating. On the surface, non-uniformly distributed Al_2O_3 particles and cracks were found. During the magnetic stirring, the flow of electrolyte caused inhomogeneities whose shape resembled loops. These inhomogenities in the coating were produced due to the high stirring rate. The chemical composition loops and "normal" coatings were similar. More Al_2O_3 particles were deposited in the composite anodic coating during anodizing with using compressed air agitation when compared to magnetic stirring.

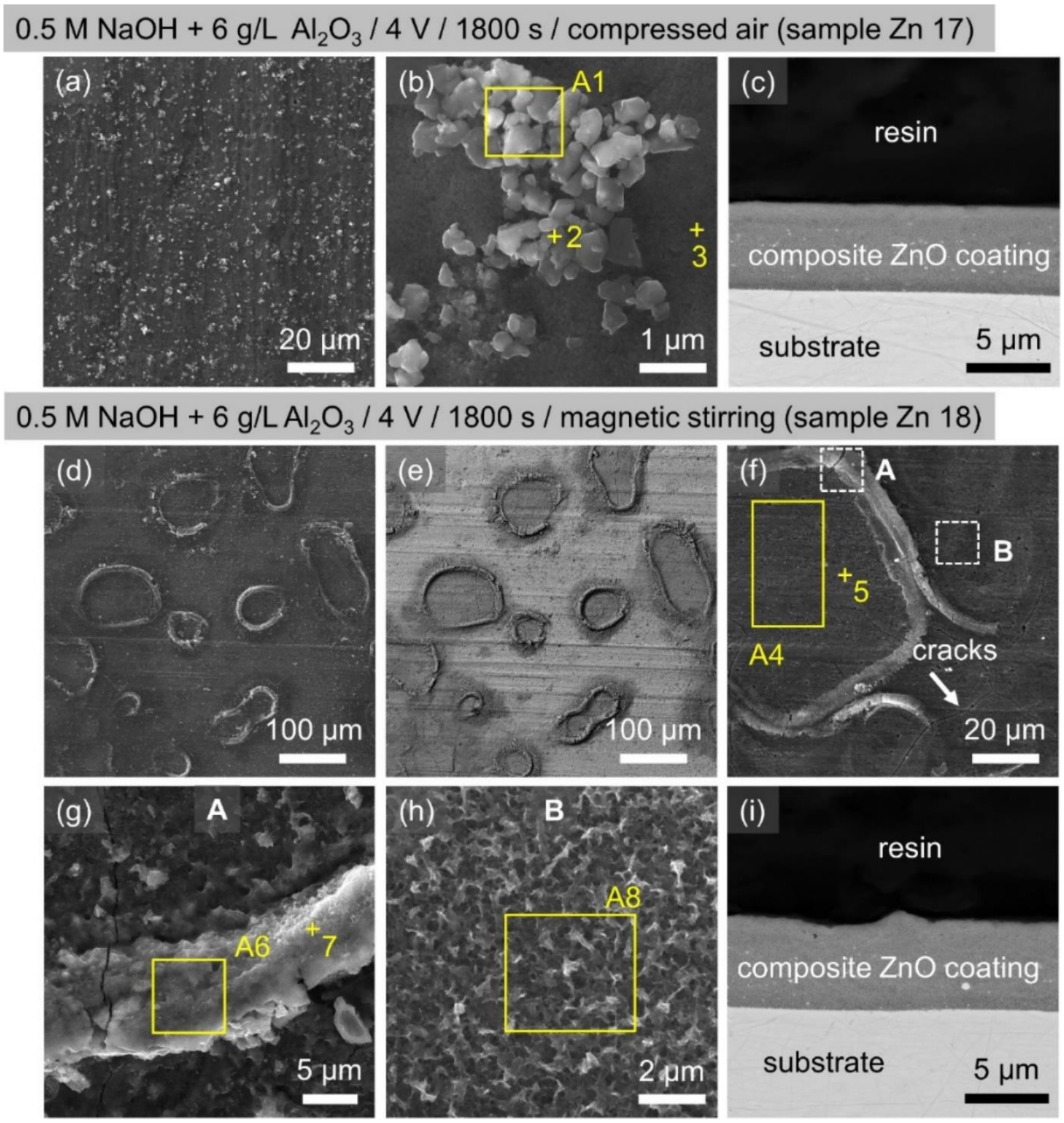

Fig. 8 *Micrographs of composite anodic coatings (a, b, d-h) top surface, and (c, i) cross-section produced in the composite electrolyte under different types of agitation of the electrolyte during anodizing; (a, b, d, f-h) SEM-SE, (c, e, i) SEM-BSE.*

4.3.3. Closing remarks on anodizing of ZnTi2 alloy

Anodizing conditions, including the type and concentration of the electrolyte, voltage, anodizing time, and the agitation mechanism on the deposition of Al_2O_3 particles from the electrolyte, have been applied to ZnTi2 substrate to produce anodic oxide coatings. The effect of the above-mentioned conditions on the resulting morphology, structure and thickness was examined, and the conclusions can be listed as follow:

Effect of applied voltage:

- The higher voltage (50 V) resulted in vigorous gas evolution during the anodizing process, which led to the appearance of horizontal cracks and gaps inside the coatings.
- Decreasing the voltage from 50 to 4 V resulted in the production of a thinner coating with a different structure and appearance. Coatings produced at 50 V in the NaOH electrolyte were white in appearance with cracks and nanorod bulk-like structure, while coatings produced at ≤ 6 V were black with porous sponge-like structure. A finer and more granular surface structure was found for coatings produced at higher voltages. Both types of coatings were polycrystalline ZnO with hexagonal (wurtzite) structure and consisted of overlapping ZnO crystalline grains.
- The applied voltage played a crucial role in determining the morphology and structure of ZnO coating and also had a more significant effect on the coating thickness than the electrolyte concentration. The structure of the formed coating is related to the appearance of the formed coating.

Effect of NaOH electrolyte concentration:

- With increasing electrolyte concentration, thicker coatings with bulk-like structure, smoother granular morphology and vertical cracks were produced.
- Electrolyte concentration affected the structure only slightly.

Effect of anodizing time:

- With increasing the anodizing time, thicker ZnO coatings were produced. At the higher anodizing voltage of 50 V, the increase in thickness was not so significant as in the case of applying the lower voltage of 4 V.

Effect of agitation mechanism on Al_2O_3 particles deposition directly from the electrolyte:

- Addition of Al_2O_3 particles directly to electrolyte did not affect the morphology and thickness of the produced composite anodic coatings.
- Using compressed air agitation during the anodizing process resulted in uniform distribution of Al_2O_3 particles in the coating.
- Using the magnetic stirring mechanism during the anodizing process had a negative effect on the deposition of non-uniform Al_2O_3 particles and on the inhomogeneous surface morphology of produced coatings.

5. Conclusions

To summarize, this thesis dealt with the development of technological process of anodizing of aluminium alloy (AA1050), pure magnesium (99.9% Mg) and zinc alloy (ZnTi2). The aim was to produce anodic coatings with higher hardness and tribological properties compared to the initial substrate and to systematically study and understand the effect of mechanical pre-treatment and individual anodizing conditions, i.e. current density/voltage, temperature, concentration and composition of the electrolyte, on the properties of produced coatings. One of the essential tasks was to prepare stable electrolyte containing Al_2O_3 particles or a mixture of Al_2O_3 and PTFE particles. This was achieved by using the SDBS (sodium dodecylbenzenesulfonate) anionic surfactant, Al_2O_3 nanoparticles and 60% PTFE suspension.

The first experimental part of the thesis is focused on aluminium alloy (AA1050), which contains intermetallic phase particles based on Al-Fe and Al-Fe-Si compounds, with irregular-shape and round-shape. The results showed that the electrolyte temperature and current density had a significant effect on the properties of produced porous anodic aluminium oxide (PAAO) coatings. Decreasing the temperature during the galvanostatic anodizing at 3 A/dm^2 in the sulfuric-oxalic acid electrolyte led to the formation of thicker and harder PAAO coatings, which however contained microcracks and hillocks on the coating surfaces. At a higher anodizing current density, the increased sulfur content suggested the incorporation of sulfate ions in the PAAO coating. In the current *vs* time curves after reaching the voltage maximum, an unusual area was recorded for the higher current densities 3 and 2 A/dm^2, which was ascribed to the incorporation of the sulfate ions in the growing coating. The porous composite AAO coating without structural defects (hillocks and microcracks) and with the best combination of mechanical properties, such as high hardness, low COF, and high wear resistance was produced by the galvanostatic anodizing process at a low current density (1 A/dm^2), and low temperature (10 °C) in an electrolyte with the addition of 6 g/L Al_2O_3 and 15 mL/L 60% PTFE suspension. Intermetallic phase particles were preferably oxidized at the low electrolyte temperature, and the oxidation rate of these phase particles was lower when a lower anodizing current density was applied.

The second set of experiments were focused on anodizing of pure magnesium in the sodium hydroxide (NaOH) electrolyte. The use of voltage had a significant effect on the morphology and thickness of the produced anodic coatings. A thicker and denser magnesium hydroxide ($Mg(OH)_2$) coating was produced with a rough surface at a lower voltage of 4 V. The coating produced in the NaOH electrolyte containing Al_2O_3 and PTFE particles at 4 V was non-compact. On the other hand, coatings produced at a higher voltage ($\geq$ 10 V) were compact and contained Al_2O_3 and PTFE particles. Further investigation and testing are necessary to be done in this area topic; for example, applying lower voltage, corrosion resistance testing and nanoindentation testing.

The final experiments were focused on anodizing of ZnTi2. Two different types of coatings were produced, referred to as “black” and “white”. Black, thinner and porous coatings with the sponge-like structure were produced at a lower voltage of 4 V in the 0.3-1 M NaOH electrolyte. White, thicker coatings composed of nanorod bulk-like structure with compact granular morphology on the surface were produced at 50 V in the 0.04 and 0.1 M NaOH electrolyte. Due to higher oxygen evolution during the anodizing process at the higher voltage, produced coatings contained horizontal cracks and gaps. The applied voltage plays an important role

in determining the morphology and appearance while higher concentrations and longer anodizing times give rise to bulk-like ZnO coatings with smaller pore size. The compressed air agitation during the anodizing process in the stable electrolyte containing 6 g/L Al_2O_3 particles led to the formation of a composite coating with uniform distribution of Al_2O_3 particles in the coating.

The anodizing process of aluminium, magnesium and zinc cannot be compared because each material requires a different pre-treatment and different anodizing conditions (i.e. type and temperature of the electrolyte, voltage/current density). Aluminium is preferably anodized in the acidic bath, commonly containing sulfuric acid, oxalic acid or their mixture, yielding a porous anodic aluminium oxide coating with parallel hexagonal pores oriented normal to the surface. At low electrolyte temperatures and high current densities, thicker and harder coatings are produced. Magnesium and zinc are preferably anodized in an alkaline electrolyte (i.e. NaOH, KOH). With increasing voltage, smoother and thinner anodic magnesium hydroxide coatings are produced. Darker anodic ZnO coatings with the sponge-like structure are produced at a low voltage and higher concentration of the NaOH electrolyte. On the other hand, white anodic ZnO coatings with bulk-like structure and horizontal cracks and gaps are produced at a high voltage and low electrolyte concentration. Addition of secondary particles (Al_2O_3 and PTFE) directly to the electrolyte have a positive effect on the hardness and tribological properties.

Although the anodizing process has been known for decades, there is still room for research and development, for both academic and industrial reasons. Further research in this field can continue; for example, anodizing of zinc is still not sufficiently described in the literature. Zinc oxide is a promising material for biomedicine, photoelectrochemical and photocatalytic applications, sensor devices and thus, systematic studies are required among others. For example, the study of the effect of current density/voltage and type, temperature, and electrolyte concentration on ZnO coating growth and morphology attract attention. Adding secondary particles directly to the electrolyte has proved to be a suitable way to achieve the required properties of produced anodic coatings, but only a few scientific papers have been published in this respect.

References

[1] SALMAN, S. A. and M. OKIDO. Anodization of magnesium (Mg) alloys to improve corrosion resistance. *Corrosion Prevention of Magnesium Alloys*. Elsevier, 2013, pp. 197-231. DOI: 10.1533/9780857098962.2.197

[2] SONG, G.-L. and Z. SHI. Anodization and corrosion of magnesium (Mg) alloys. *Corrosion Prevention of Magnesium Alloys*. Elsevier, 2013, pp. 232-281. DOI: 10.1533/9780857098962.2.197

[3] GOUEFFON, Y., L. ARURAULT, C. MABRU, C. TONON and P. GUIGUE. Black anodic coatings for space applications: Study of the process parameters, characteristics and mechanical properties. *Journal of Materials Processing Technology*. 2009, vol. 209, no. 11, pp. 5145-5151. DOI: 10.1016/j.jmatprotec.2009.02.013

[4] BRALLA, J. G. *Handbook of manufacturing processes: how products, components and materials are made*. New York: Industrial Press, 2007. ISBN 9780831131791.

[5] GROOVER, M. P. *Fundamentals of modern manufacturing: materials, processes and systems*. New York: Wiley Global Education, 2012. ISBN 9781118476550.

[6] VOON, C. H., M. N. DERMAN, U. HASHIM, B. Y. LIM, S. T. SAM, K. L. FOO and S. T. TEN. Synthesis of Nanoporous Zinc Oxide by Anodizing of Zinc in Distilled Water. *Applied Mechanics and Materials*. 2015, vol. 754-755, pp. 1126-1130. DOI: 10.4028/www.scientific.net/AMM.754-755.1126

[7] SULKA, G. D. Highly Ordered Anodic Porous Alumina Formation by Self-Organized Anodizing. *Nanostructured Materials in Electrochemistry*. Weinheim, Germany: Wiley-VCH Verlag, 2008. ISBN 9783527621507. DOI: 10.1002/9783527621507.ch1

[8] EDITED BY H. DONG. *Surface engineering of light alloys aluminium, magnesium and titanium alloys*. Boca Raton: CRC Press, 2010. ISBN 9781845699451.

[9] JIANG, B. L. and Y. F. GE. Micro-arc oxidation (MAO) to improve the corrosion resistance of magnesium (Mg) alloys. *Corrosion Prevention of Magnesium Alloys*. Elsevier, 2013, pp. 163-196. DOI:10.1533/9780857098962.2.163

[10] CHEN, S., C. KANG, J. WANG, C. LIU and K. SUN. Synthesis of anodizing composite films containing superfine Al2O3 and PTFE particles on Al alloys. *Applied Surface Science*. 2010, vol. 256, no. 22, pp. 6518-6525. DOI: 10.1016/j.apsusc.2010.04.040

[11] XIA, G., H. JIANG, R. LIU and Y. ZHAI. Effects of surfactant on the stability and thermal conductivity of Al2O3/de-ionized water nanofluids. *International Journal of Thermal Sciences*. 2014, vol. 84, pp. 118-124. DOI: 10.1016/j.ijthermalsci.2014.05.004

[12] LI, S., M. ZHU, J. LIU, M. YU, L. WU, J. ZHANG and H. LIANG. Enhanced tribological behavior of anodic films containing SiC and PTFE nanoparticles on Ti6Al4V alloy. *Applied Surface Science*. 2014, vol. 316, pp. 28-35. DOI: 10.1016/j.apsusc.2014.07.088

[13] REMEŠOVÁ, M., L. KLAKURKOVÁ, M. HORYNOVÁ, L. ČELKO and J. KAISER. Preparation of Metallographic Samples with Anodic Layers. *Materials Science Forum*. 2017, vol. 891, pp. 106-110. DOI: 10.4028/www.scientific.net/MSF.891.106

[14] GASTÓN-GARCÍA, B., E. GARCÍA-LECINA, J. A. DÍEZ, M. BELENGUER and C. MÜLLER. Local Burning Phenomena in Sulfuric Acid Anodizing: Analysis of Porous Anodic Alumina Layers on AA1050. *Electrochemical and Solid-State Letters*. 2010, vol. 13, no. 11. DOI: 10.1149/1.3478482

[15] JARIYABOON, M., P. MØLLER, R.E. DUNIN-BORKOWSKI and R. AMBAT. FIB-SEM investigation of trapped intermetallic particles in anodic oxide films on AA1050 aluminium. *Anti-Corrosion Methods and Materials*. 2011, vol. 58, no. 4, pp. 173-178. DOI: 10.1108/00035591111148885

[16] MONTERO-MORENO, J. M., M. SARRET and C. MÜLLER. Self-ordered porous alumina by two-step anodizing at constant current: Behaviour and evolution of the structure. *Microporous and Mesoporous Materials*. 2010, vol. 136, no. 1-3, pp. 68-74. DOI: 10.1016/j.micromeso.2010.07.022

[17] KOROLEVA, E., G. E. THOMPSON, G. HOLLRIGL and M. BLOECK. Surface morphological changes of aluminium alloys in alkaline solution. *Corrosion Science*. 1999, vol. 41, no. 8, pp. 1475-1495. DOI: 10.1016/S0010-938X(98)00188-7

[18] SULKA, G. D., S. STROOBANTS, V. MOSHCHALKOV, G. BORGHS and J.-P. CELIS. Synthesis of Well-Ordered Nanopores by Anodizing Aluminum Foils in Sulfuric Acid. *Journal of The Electrochemical Society*. 2002, vol. 149, no. 7. DOI: 10.1149/1.1481527

[19] MICHALSKA-DOMAŃSKA, M., M. NOREK, W. J. STĘPNIOWSKI and B. BUDNER. Fabrication of high quality anodic aluminum oxide (AAO) on low purity aluminium-A comparative study with the AAO produced on high purity aluminum. *Electrochimica Acta*. 2013, vol. 105, pp. 424-432. DOI: 10.1016/j.electacta.2013.04.160

[20] PARKHUTIK, V. P., J. M. ALBELLA, Y. E. MAKUSHOK, I. MONTERO, J. M. MARTINEZ-DUART and V. I. SHERSHULSKII. Study of aluminium anodization in sulphuric and chromic acid solutions—I. Kinetics of growth and composition of oxides. *Electrochimica Acta*. 1990, vol. 35, no. 6, pp. 955-960. DOI: 10.1016/0013-4686(90)90027-W

[21] HAKIMIZAD, A., K. RAEISSI and F. ASHRAFIZADEH. Characterization of aluminum anodized layers modified in sulfuric and phosphoric acid baths and their effect on conventional electrolytic coloring. *Surface and Coatings Technology*. 2012, vol. 206, no. 8-9, pp. 2438-2445. DOI: 10.1016/j.surfcoat.2011.10.046

[22] FRATILA-APACHITEI, L. E., H. TERRYN, P. SKELDON, G. E. THOMPSON, J. DUSZCZYK and L. KATGERMAN. Influence of substrate microstructure on the growth of anodic oxide layers. *Electrochimica Acta*. 2004, vol. 49, no. 7, pp. 1127-1140. DOI: 10.1016/j.electacta.2003.10.024

[23] THEOHARI, S. and C. KONTOGEORGOU. Effect of temperature on the anodizing process of aluminum alloy AA 5052. *Applied Surface Science*. 2013, vol. 284, pp. 611-618. DOI: 10.1016/j.apsusc.2013.07.141

[24] GUEZMIL, M., W. BENSALAH, A. KHALLADI, K. ELLEUCH, M. DEPETRIS-WERY and H.F. AYEDI. Friction coefficient and microhardness of anodized aluminum alloys under different elaboration conditions. *Transactions of Nonferrous Metals Society of China*. 2015, vol. 25, no. 6, pp. 1950-1960. DOI: 10.1016/S1003-6326(15)63803-1

[25] WEI, P.-S. and T.-S. SHIH. Monitoring the Progressive Development of an Anodized Film on Aluminum. *Journal of The Electrochemical Society*. 2007, vol. 154, no. 11. DOI: 10.1149/1.2780864

[26] AERTS, T., I. DE GRAEVE and H. TERRYN. Study of initiation and development of local burning phenomena during anodizing of aluminium under controlled convection. *Electrochimica Acta*. 2008, vol. 54, no. 2, pp. 270-279. DOI: 10.1016/j.electacta.2008.08.004

[27] LOSIC, D. and A. SANTOS, ed. *Nanoporous Alumina: Fabrication, Structure, Properties and Applications*. Springer. 2015, vol. 219. DOI: 10.1007/978-3-319-20334-8.

[28] REMEŠOVÁ, M., S. TKACHENKO, D. KVARDA, I. ROČŇÁKOVÁ, B. GOLLAS, M. MENELAOU, L. ČELKO and J. KAISER. Effects of anodizing conditions and the addition of Al2O3/PTFE particles on the microstructure and the mechanical properties of porous anodic coatings on the AA1050 aluminium alloy. *Applied Surface Science*. 2020, vol. 513. DOI: 10.1016/j.apsusc.2020.145780

[29] MOUTARLIER, V, M. P GIGANDET, J. PAGETTI and B. NORMAND. Influence of oxalic acid addition to chromic acid on the anodising of Al 2024 alloy. *Surface and Coatings Technology*. 2004, vol. 182, no. 1, pp. 117-123. DOI: 10.1016/S0257-8972(03)00875-2

[30] FRATILA-APACHITEI, L. E., J. DUSZCZYK and L. KATGERMAN. Vickers microhardness of AlSi(Cu) anodic oxide layers formed in H2SO4 at low temperature. *Surface and Coatings Technology*. 2003, vol. 165, no. 3, pp. 309-315. DOI: 10.1016/S0257-8972(02)00750-8

[31] ROA, J. J., B. GASTÓN-GARCÍA, E. GARCÍA-LECINA and C. MÜLLER. Mechanical properties at nanometric scale of alumina layers formed in sulphuric acid anodizing under burning conditions. *Ceramics International*. 2012, vol. 38, no. 2, pp. 1627-1633. DOI: 10.1016/j.ceramint.2011.09.053

[32] ZHANG, P. and Y. ZUO. Effects of pore parameters on performance of anodic film on 2024 aluminum alloy. *Materials Chemistry and Physics*. 2019, vol. 231, pp. 9-20. DOI: 10.1016/j.matchemphys.2019.04.008

[33] CHUNG, I. C., C. K. CHUNG and Y. K. SU. Effect of current density and concentration on microstructure and corrosion behavior of 6061 Al alloy in sulfuric acid. *Surface and Coatings Technology*. 2017, vol. 313, pp. 299-306. DOI: 10.1016/j.surfcoat.2017.01.114

[34] ZHANG, D., Y. GOU, Y. LIU and X. GUO. A composite anodizing coating containing superfine Al2O3 particles on AZ31 magnesium alloy. *Surface and Coatings Technology*. 2013, vol. 236, pp. 52-57. DOI: 10.1016/j.surfcoat.2013.04.059

[35] LIANG, J., L. HU and J. HAO. Preparation and characterization of oxide films containing crystalline TiO2 on magnesium alloy by plasma electrolytic oxidation. *Electrochimica Acta*. 2007, vol. 52, no. 14, pp. 4836-4840. DOI: 10.1016/j.electacta.2007.01.059

[36] CHEN, M. H., K. C. KAO, M. W. TU and D. N. ZHANG. Self-Lubricating SiC/PTFE Composite Coating Formation on Surface of Aluminium Alloy. *Advanced Materials Research*. 2012, vol. 490-495, pp. 3511-351. DOI: 10.4028/www.scientific.net/AMR.490-495.3511

[37] ESCOBAR, J., L. ARURAULT and V. TURQ. Improvement of the tribological behavior of PTFE-anodic film composites prepared on 1050 aluminum substrate. *Applied Surface Science*. 2012, vol. 258, no. 20, pp. 8199-8208. DOI: 10.1016/j.apsusc.2012.05.022

[38] LU, J., G. WEI, Y. YU, C. GUO and L. JIANG. Aluminum alloy AA2024 anodized from the mixed acid system with enhanced mechanical properties. *Surfaces and Interfaces*. 2018, vol. 13, pp. 46-50. DOI: 10.1016/j.surfin.2018.08.003

[39] Páleníček, M., M. Papula, M. Remešová, D. Jech, I. Ročňáková and L. Čelko. Anodizing of Pure Magnesium in Sodium Hydroxide Electrolyte Solution. In Metallography and Fractography XVII. Materials Science Forum. Switzerland: Trans Tech Publications Ltd. 2019. ISBN: 978-3-0357-1018-2, in press.

[40] SALMAN, S. A., R. MORI, R. ICHINO and M. OKIDO. Effect of Anodizing Potential on the Surface Morphology and Corrosion Property of AZ31 Magnesium Alloy. *Materials transactions*. 2010, vol. 51, no. 6, pp. 1109-1113. DOI: 10.2320/matertrans.M2009380

[41] SALMAN, S. A., R. ICHINO and M. OKIDO. A Comparative Electrochemical Study of AZ31 and AZ91 Magnesium Alloy. *International Journal of Corrosion*. 2010, pp. 1-7. DOI: 10.1155/2010/412129

[42] KIM, S.-J., M. OKIDO, Y. MIZUTANI, R. ICHINO, S. TANIKAWA and S. HASEGAWA. Formation of Anodic Films on Mg-Al Alloys in NaOH solutions at Constant Potentials. *Materials transactions*. 2003, vol. 44, no. 5, pp. 1036-1041. DOI: 10.2320/matertrans.44.1036

[43] KIM, S. J. and M. OKIDO. The electrochemical properties and mechanism of formation of anodic oxide films on Mg-Al alloys. *Bulletin-Korean chemical society*. 2003, vol. 24, no. 8, pp. 975-980. DOI: 10.5012/bkcs.2003.24.7.975

[44] MABON, J.C. and O.T. INAL. Optimization and evaluation of black zinc selective solar absorber surfaces. *Thin Solid Films*. 1984, vol. 115, no. 1, pp. 51-73. DOI: 10.1016/0040-6090(84)90316-X

[45] ROCCA, E., D. VEYS-RENAUX and K. GUESSOUM. Electrochemical behavior of zinc in KOH media at high voltage: Micro-arc oxidation of zinc. *Journal of Electroanalytical Chemistry*. 2015, vol. 754, pp. 125-132. DOI: 10.1016/j.jelechem.2015.06.021

[46] ZHANG, X. G. *Corrosion and electrochemistry of zinc*. New York: Plenum Press, 1996. ISBN 0306453347.

[47] MIKA, K., R. P. SOCHA, P. NYGA, E. WIERCIGROCH, K. MALEK, M. JAROSY, T. UCHACY, G. S. SULKA and L. ZARASKA Electrochemical synthesis and characterization of dark nanoporous zinc oxide films. *Electrochimica Acta*. 2019, vol. 305, pp. 349-359. DOI: 10.1016/j.electacta.2019.03.052

[48] DONG, J., Z. LIU, J. DONG, D. ARIYANTI, Z. NIU, S. HUANG, W. ZHANG and W. GAO. Self-organized ZnO nanorods prepared by anodization of zinc in NaOH electrolyte. *RSC Advances*. 2016, vol. 6, no. 77, pp. 72968-72974. DOI: 10.1039/C6RA16995C

List of authors scientific achievements

Authors scientific identifiers

Research ID: G-9563-2014
ORCID ID: 0000-0003-1678-5618

A.1. Publications in impact journal

REMEŠOVÁ, M.; TKACHENKO, S.; KVARDA, D.; ROČŇÁKOVÁ, I.; GOLLAS, B.; MENELAOU, M.; ČELKO, L.; KAISER, J. Effects of anodizing conditions and the addition of Al2O3/PTFE particles on the microstructure and the mechanical properties of porous anodic coatings on the AA1050 aluminium alloy. *Applied Surface Science,* 2020. DOI: 10.1016/j.apsusc.2020.145780

SLÁMEČKA, K.; JECH, D.; KLAKURKOVÁ, L; TKACHENKO, S.; REMEŠOVÁ, M.; GEJDOŠ, P.; ČELKO, L. Thermal cycling damage in pre-oxidized plasma-sprayed MCrAlY + YSZ thermal barrier coatings: Phenomenon of multiple parallel delamination of the TGO layer. *Surface and Coatings Technology*. 2020. DOI: 10.1016/j.surfcoat.2019.125328

HORYNOVÁ, M.; REMEŠOVÁ, M.; KLAKURKOVÁ, L.; DVOŘÁK, K.; ROČŇÁKOVÁ, I.; YAN, S.; ČELKO, L.; SONG, G. L. Design of tailored biodegradable implants: The effect of voltage on electrodeposited calcium phosphate Coatings on pure magnesium. *Journal of the American Ceramic Society,* 2019, pp. 123-135. DOI: 10.1111/jace.15888

ČELKO, L.; MENELAOU, M.; CASAS LUNA, M.; HORYNOVÁ, M.; MUSÁLEK, T.; REMEŠOVÁ, M.; DÍAZ DE LA TORRE, S.; MORSI, K.; KAISER, J. Spark Plasma Extrusion and the Thermal Barrier Concept. *Metallurgical and materials transactions B-processing science, 2*019, pp. 656-665. DOI: 10.1007/s11663-018-1493-3

ROČŇÁKOVÁ, I.; SLÁMEČKA, K.; MONTUFAR JIMENEZ, E.; REMEŠOVÁ, M.; DYČKOVÁ, L.; BŘÍNEK, A.; JECH, D.; DVOŘÁK, K.; ČELKO, L.; KAISER, J. Deposition of Hydroxyapatite and Tricalcium Phosphate Coatings by Suspension Plasma Spraying: Effects of Torch Speed. *Journal of the European Ceramic Society,* 2018, pp. 5489-5496. DOI: 10.1016/j.jeurceramsoc.2018.08.007

KLAKURKOVÁ, L.; HORYNOVÁ, M.; JULIŠ, M.; GEJDOŠ, P.; SKALKA, P.; REMEŠOVÁ, M.; ČELKO, L. Failure analysis of massively failed compressed air cartridge. *Engineering failure analysis,* 2017, pp. 776-782. DOI: 10.1016/j.engfailanal.2017.07.016

SLÁDKOVÁ, L.; PROCHAZKA, D.; POŘÍZKA, P.; ŠKARKOVÁ, P.; REMEŠOVÁ, M.; HRDLIČKA, A.; NOVOTNÝ, K.; ČELKO, L.; KAISER, J. Improvement of the Laser-Induced Breakdown Spectroscopy method sensitivity by the usage of combination of Ag-nanoparticles and vacuum conditions. *Spectrochimica Acta Part B,* 2017, pp. 48-55. DOI: 10.1016/j.sab.2016.11.005

A.2. Selected contributions to conference proceedings indexed in WoS or Scopus

JECH, D.; REMEŠOVÁ, M.; KOMAROV, P.; TKACHENKO, S.; ČESÁNEK, Z.; SCHUBERT, J.; HOUDKOVÁ, Š.; ČELKO, L. Evaluation of Microstructure, Phase Composition and Hardness of Alternative Abradable Ceramic Coating Systems Produced by Means of Atmospheric Plasma Spraying. In *Binders, Materials and Technologies in Modern Construction V. Solid State Phenomena.* Switzerland: Trans Tech Publications, 2019, pp. 161-166. ISSN: 1662-9779.

REMEŠOVÁ, M.; KLAKURKOVÁ, L.; ROČŇÁKOVÁ, I.; DYČKOVÁ, L.; ČELKO, L.; KAISER, J. Application of Metallographic Analysis Techniques for Detection and Identification of Spray Paint Defects. In *Přínos metalografie pro řešení výrobních problémů. Solid State Phenomena.* 14. Switzerland: Trans Tech Publications, 2017, pp. 118-123. ISSN: 1662-9779.

DYČKOVÁ, L.; KLAKURKOVÁ, L.; GEJDOŠ, P.; REMEŠOVÁ, M.; JULIŠ, M.; ČELKO, L. Causal analysis of damage of a cover. In *Přínos metalografie pro řešení výrobních problémů. Solid State Phenomena.* 14. Switzerland: Trans Tech Publications, 2017, pp. 57-62. ISSN: 1662-9779.

HORYNOVÁ, M.; REMEŠOVÁ, M.; KLAKURKOVÁ, L.; JULIŠ, M.; GEJDOŠ, P.; DYČKOVÁ, L. Evaluation of surface degradation of deoxidized AW-AlMg0.7Si alloy. In *Přínos metalografie pro řešení výrobních problémů. Solid State Phenomena.* 14. Switzerland: Trans Tech Publications, 2017, pp. 136-141. ISSN:1662-9779.

REMEŠOVÁ, M.; KLAKURKOVÁ, L.; HORYNOVÁ, M.; ČELKO, L.; KAISER, J. Preparation of Metallographic Samples with Anodic Layers. In *Metallography XVI. Materials Science Forum.* Switzerland: Trans Tech Publications Ltd., 2017, pp. 106-110. ISSN: 0255-5476.

REMEŠOVÁ, M.; KLAKURKOVÁ, L.; ČELKO, L.; SLÁDKOVÁ, L.; JECH, D.; KAISER, J. Anodizing of Zinc-Titanium Alloy in NaOH and KOH Baths. In *Materials Structure & Micromechanics of Fracture VIII. Solid State Phenomena.* Solid State Phenomena. Switzerland: Trans Tech Publications, 2017, pp. 399-402. ISSN: 1012-0394.

A.3. Active conferences, workshops and internship

14th Conference on Contribution of Metallography to Production Problem Solutions, Mariánské Lázně, Czech Republic, 2017

International Conference on Materials Structure and Micromechanics of Fracture, Brno, Czech Republic, 2016

16th International Symposium on Metallography and Materials Science in Slovakia, 2016

International Conference on Engineering Failure Analysis, Leipzig, Germany, 2016

International workshop, Progressive and non-traditional technologies of surface treatment, Brno, Czech Republic, 2018

Nanoindentation workshop, CEITEC Nano RI, Brno, Czech Republic, 2017

International workshop, Progressive and non-traditional technologies of surface treatment, Brno, Czech Republic, 2017

International workshop, Progressive and non-traditional technologies of surface treatment, Brno, Czech Republic, 2016

Electrochemistry workshop, COST MP 1407, Cracow, Poland, 2015

4.2.-30.4.2019 Erasmus+ Traineeship, Institute for Chemistry and Technology of Materials, Graz University of Technology, traineeship title: *Activation of aluminium electrodes in deep eutectic solvents*, coordinator - Assoc. Prof. Dr. Bernhard Gollas

A.4. Participation in research projects

Student project STI-J-18-5308, Brno University of Technology, CEITEC, Czech Republic, Výzkum a vývoj technologie anodické oxidace hliníkové slitiny EN AW-1050A za účelem přípravy dopovaných konverzních vrstev, coordinator - Prof. Jozef Kaiser

MPO no. FV20232 Biodegradovatelné strukturované implantáty vyrobené metodou 3D tisku kovů - MPO, FV - TRIO

MPO no. FV10897 VaV speciálních typů brusiv pro broušení ložiskových kroužků se zaměřením dodržení požadované integrity broušení oběžných drah - MPO, FV – TRIO

MPO no. FV30335 Výzkum a vývoj pokročilých typů pojiv pro speciální brousicí nástroje - MPO, FV - TRIO

GAČR no. 19-22662S In situ precipitace hydroxyapatitu uvnitř hierarchických titanových struktur - GAČR

MPO no. FV10477 Technologie kombinovaného zdroje plasmatu pro vznik pokročilých povrchových úprav MPO, FV - TRIO